

Central Lancashire Online Knowledge (CLoK)

Title	A search for HI in five elliptical galaxies with fine structure
Type	Article
URL	https://clok.uclan.ac.uk/id/eprint/205/
DOI	https://doi.org/10.1086/345822
Date	2003
Citation	Hibbard, JE and Sansom, Anne E (2003) A search for HI in five elliptical
	galaxies with fine structure. Astronomical Journal, 125 (2). pp. 667-683.
	ISSN 0004-6256
Creators	Hibbard, JE and Sansom, Anne E

It is advisable to refer to the publisher's version if you intend to cite from the work. https://doi.org/10.1086/345822

For information about Research at UCLan please go to http://www.uclan.ac.uk/research/

All outputs in CLoK are protected by Intellectual Property Rights law, including Copyright law. Copyright, IPR and Moral Rights for the works on this site are retained by the individual authors and/or other copyright owners. Terms and conditions for use of this material are defined in the http://clok.uclan.ac.uk/policies/

A SEARCH FOR H 1 IN FIVE ELLIPTICAL GALAXIES WITH FINE STRUCTURE

J. E. Hibbard

National Radio Astronomy Observatory, 520 Edgemont Road, Charlottesville, VA 22903; jhibbard@nrao.edu

AND

A. E. Sansom

Centre for Astrophysics, University of Central Lancashire, Preston PR12HE, UK; AESansom@uclan.ac.uk
Received 2002 August 14; accepted 2002 October 30

ABSTRACT

We report on VLA H I spectral line observations of five early-type galaxies classified as optically peculiar because of the presence of jets, ripples, or other optical fine structure. We detect H I within the primary beam (30' half-power beamwidth) in four of the five systems. However, in only one case is this gas associated with the targeted elliptical galaxy. In the other cases the H I is associated with a nearby gas-rich disk or dwarf galaxy. The one H I detection is for NGC 7626, where we tentatively detect an H I cloud lying between 20 and 40 kpc southwest of the galaxy center. Its origin is unclear. Our failure to detect obvious tidal H I features suggests that if these fine-structure elliptical galaxies are remnants of disk galaxy mergers, either the progenitors were gas-poor or they are well evolved and any gaseous tidal features have dispersed and/or been converted into other phases. Our targeted systems all reside in groups or clusters, and it seems likely that tidal H I is shorter lived in these environments than suggested by studies of more isolated merger remnants.

Key words: galaxies: individual (NGC 3610, NGC 3640, NGC 4382, NGC 5322, NGC 7626) — galaxies: interactions — galaxies: ISM — galaxies: peculiar

1. INTRODUCTION

It was once believed that elliptical galaxies were evolved objects with simple morphologies. However, early image processing techniques revealed that anywhere from onefourth to one-third of such galaxies exhibit faint morphological peculiarities in the form of shells, ripples, and extended plumes (Malin 1978, 1979; Malin & Carter 1980, 1983; Schweizer & Ford 1984; Schweizer & Seitzer 1988, 1992, hereafter SS92; Reid, Boisson, & Sansom 1994). Numerical work soon demonstrated that such features could be reproduced either by small accretion events (Quinn 1984; Dupraz & Combes 1986; Hernquist & Quinn 1988, 1989) or by major mergers (Hernquist & Spergel 1992; Hibbard & Mihos 1995). The appearance of such features in heretofore "normal" elliptical galaxies is seen as strong support for the Toomre merger hypothesis that (some) elliptical galaxies evolve from the merger of disk galaxies (Toomre & Toomre 1972; Toomre 1977).

In an effort to quantify the frequency and quantity of such morphological peculiarities, Schweizer et al. (1990) introduced a fine-structure index, Σ , which increases with the number of morphological peculiarities (for detailed review, see Schweizer 1998). Statistically, galaxies with larger values of Σ have observational characteristics (colors and spectral line strengths) consistent with the presence of younger stellar populations, supporting the idea that they represent more recent mergers in which starbursts have occurred (Schweizer et al. 1990; SS92). This association suggests that the fine-structure index might provide a means to locate evolved merger remnants lying in the so-called King gap between \sim 1 Gyr old remnants and old elliptical galaxies (I. King, quoted in Toomre 1977).

However, some recent studies have called into question the identification of elliptical galaxies with large amounts of fine structure as aged merger remnants (Silva & Bothun 1998a, 1998b). Since such subtle morphological peculiarities may arise from less structurally damaging events, such as accretions, they are not unambiguous signatures of major mergers. To remove this ambiguity, it is desirable to find a more direct link between a high fine-structure index and a merger origin.

Some clues as to the expected appearance of "King gap" objects are provided by observations of nearby systems that are undeniably the remnants of disk-disk mergers. The best examples of such objects are the last two members of the Toomre sequence (Toomre 1977), a proposed evolutionary sequence of disk-disk mergers. These two systems, NGC 3921 and NGC 7252, are evolved merger remnants with single nuclei, postburst stellar populations, relaxed $r^{1/4}$ light profiles, and dynamical ages of \sim 0.5–1 Gyr (Schweizer 1982, 1996; Schweizer et al. 1996; Hibbard & Mihos 1995; Miller et al. 1997; Hibbard & Yun 1999). H I mapping of these systems with the VLA¹ shows their tidal tails to be rich in atomic hydrogen (Hibbard et al. 1994; Hibbard & van Gorkom 1996), firmly establishing their status as diskmerger products.

Both remnants are also found to have a very low central H I content. This result is somewhat surprising, not only in view of large amounts of H I that must have been sent into the central regions during the early stages of merging (e.g., Barnes & Hernquist 1991), but also in view of the atomic gas-rich material that is observed streaming back into the remnant bodies from the tidal tails (Hibbard & Mihos 1995; Yun & Hibbard 2001). These studies suggest that as the merger evolves the remnant should have a decreasing amount of fine structure, decreasing amounts of both inner and outer tidal gas, and a multiepoch aging stellar population.

¹ The VLA of the National Radio Astronomy Observatory is operated by Associated Universities, Inc., under cooperative agreement with the National Science Foundation.

The present study is an attempt to locate products of gasrich mergers intermediate in age between recent merger remnants such as NGC 3921 and NGC 7252 and elliptical galaxies with less obvious peculiarities. H I mapping of morphologically peculiar early-type galaxies provides strong evidence pointing to a gas-rich merger origin for a number of objects (e.g., Schiminovich et al. 1994, 1995; Schiminovich 2001; Lim & Ho 1999; Balcells et al. 2001; Chang et al. 2001). With this in mind, we have targeted five elliptical galaxies with varying amounts of optical fine structure $(\Sigma = 2.0-7.6)$ for H I mapping observations with the VLA in its most compact configuration (D array) to look for the remnants of gas-rich tidal features in the outer regions. The five systems are NGC 3610, 3640, 4382, 5322, and 7626. In this paper we report the results of the H_I observations of these five galaxies.

The present paper is structured as follows. In \S 2 we describe the selection criterion used to define the targets for this study. In \S 3 we describe the VLA observations and data reduction. In \S 4 we describe the results for each of the five systems, and in \S 5 we discuss these results. Finally we summarize our conclusions in \S 6.

2. SAMPLE SELECTION

The galaxies for this study were chosen from the sample of 69 field elliptical and S0 galaxies for which the fine-structure index has been tabulated by SS92. The fine-structure index is defined as $\Sigma = S + \log(1+n) + J + B + X$, where S is a visual estimate of the strength of the most prominent ripples, n is the number of detected ripples, J is the number of luminous plumes or "jets," B is a visual estimate of the maximum boxiness of isophotes, and X indicates the absence or presence of an X-structure. The well-known young (\sim 0.5–1 Gyr) merger remnants NGC 3921 and NGC 7252 have $\Sigma = 8.8$ and 10.1, respectively, while the sample of field S0s and elliptical galaxies studied by SS92 have values in the range $\Sigma = 0$ –7.6.

The five galaxies chosen for this study are listed in Table 1, along with their basic properties, group membership, fine-structure index, and observational details. We selected the three galaxies in the list of SS92 with the highest values of Σ (NGC 3610, 3640, and 4382). We originally chose galaxies to also cover a range of X-ray excess $(L_{\rm X}/$ L_B), so that we might address whether merger remnants "grow" X-ray halos as tidal gas falls back toward the remnant (Hibbard et al. 1994; Fabbiano & Schweizer 1995; Read & Ponman 1998). However, a reanalysis of the ROSAT X-ray data for these systems (Sansom, Hibbard, & Schweizer 2000) shows that all but NGC 7626 are in the lowest X-ray class, so we will not address this question here. In an earlier study (Sansom et al. 2000), we used the present sample along with the early-type galaxies in the list of SS92 that have existing X-ray observations to test the hypothesis that X-ray halos form as cold tidal gas falls back into the remnant bodies. We found no clear trends, other than the previously reported trend for recent merger remnants to be X-ray faint (Fabbiano & Schweizer 1995; Georgakakis, Forbes, & Norris 2000; O'Sullivan, Forbes, & Ponman 2001).

3. VLA DATA

The neutral hydrogen data were collected in 1997 December by using the VLA in its spectral line mapping mode. The

array was in its most compact D-array configuration, providing maximum sensitivity to extended emission. Five galaxies and several calibrators were observed. Table 1 gives a log of these observations.

Since the atomic gas within tidal debris typically has narrow line widths ($\sigma_v \sim 5{\text -}10 \text{ km s}^{-1}$; Hibbard et al. 1994; Hibbard & van Gorkom 1996), the correlator mode was chosen to give the smallest channel spacing while still covering the expected range of velocities for tidal gas. We therefore chose the 2AC mode with on-line Hanning smoothing and a 3.125 MHz bandwidth, resulting in 63 spectral channels each of width ~ 10.4 km s⁻¹ and a total velocity coverage of \sim 650 km s⁻¹. This is sufficient to cover the spread of velocities observed in other peculiar elliptical galaxies $(\sim 500 \text{ km s}^{-1}, \text{ e.g., Schiminovich et al. } 1994, 1995, 2001).$ However, most of the target elliptical galaxies are members of loose groups or clusters (see § 4) and the present observations do not cover the velocity range of all group or cluster members. The field of view is set by the 25 m diameter of the individual array elements and amounts to a half-power beamwidth (HPBW) of 30'. Our on-source integration time of \sim 2 hours per source provides an rms noise of \sim 0.6 mJy beam⁻¹, corresponding to a 3 σ column density sensitivity of $\sim 7 \times 10^{18}$ cm⁻² per channel over a typical beam size of $60'' \times 50''$ (see Table 1).

The data were reduced using the Astronomical Image Processing System (AIPS) software. For each observation the absolute flux level was set by observing a standard VLA flux calibrator. The antenna phases were calibrated with observations of an unresolved continuum source before and after each galaxy observation. The bandpass was calibrated using either the flux or phase calibrator, whichever provided the highest signal-to-noise ratio. For details on VLA observation and calibration techniques, see Taylor, Carilli, & Perley (1999). For the specifics of spectral line data reduction and imaging, see Rupen (1999).

The spectral response of the VLA resulted in 55 usable channels (channels 3–57) out of the 63 channel data cubes. The continuum was removed using an iterative procedure that involved subtracting linear fits to the visibilities at either end of the passband. Various combinations of channels were used in the fit, and the resulting data cube was mapped and reviewed to determine the range of line-free channels. In cases in which H I was detected from a companion at velocities significantly different from the central velocity setting, separate data cubes were made using the appropriate line-free channels for continuum subtraction.

The data were mapped using a ROBUST weighting parameter of +1 (Briggs 1995), which provides good sensitivity to faint extended emission. Continuum intensity and continuum-subtracted line maps were made of the entire primary beam. The line maps were cleaned using the standard methods in AIPS. To further increase our sensitivity, we smoothed the data first in velocity by a factor of 4, then spatially by convolving to a resolution of 90". No further detections were made in either of the smoothed data sets, and all figures presented here use the full resolution data cubes.

Neutral hydrogen masses are calculated according to the equation $M_{\rm H\,I}=2.36\times 10^5 D_{\rm Mpc}^2 \int S_{\rm H\,I} dv$, where $D_{\rm Mpc}$ is the distance to the source in megaparsecs, $S_{\rm H\,I}$ is the continuum-subtracted H I line specific intensity in janskys, and v is the velocity expressed in kilometers per second. The integral is over the line, assuming the atomic gas to be optically thin.

SAMPLE PROPERTIES TABLE 1

E5: E6: A(8)0+pec E729 178 29.2 6.85 7.6 6.85 LGG 234 (NGC 3642 Group) LGG 233 (NGC 3640 Group) LGG 292 (Virgo I Group) LGG 360 (NGC 3642 Group) LGG 233 (NGC 3640 Group) LGG 292 (Virgo I Group) LGG 360 (NGC 3642 Group) LGG 233 (NGC 3640 Group) LGG 292 (Virgo I Group) LGG 360 (NGC 3642 Group) LGG 233 (NGC 3640 Group) LGG 292 (Virgo I Group) LGG 360 (NGC 3640 Group) LGG 292 (Virgo I Group) LGG 360 (NGC 3640 Group) LGG 292 (Virgo I Group) LGG 360 (NGC 3640 Group) LGG 292 (Virgo I Group) LGG 360 (NGC 3640 Group) LGG 292 (Virgo I Group) LGG 360 (NGC 3640 Group) LGG 292 (Virgo I Group) LGG 360 (NGC 3640 Group) LGG 292 (Virgo I Group) LGG 360 (NGC 3640 Group) LGG 292 (Virgo I Group) LGG 360 (NGC 3640 Group) LGG 292 (Virgo I Group) LGG 360 (NGC 3640 Group) LGG 292 (Virgo I Group) LGG 360 (NGC 3640 Group) LGG 292 (Virgo I Group) LGG 360 (NGC 3640 Group) LGG 292 (Virgo I Group) LGG 360 (NGC 3640 Group) LGG 292 (Virgo I Group) LGG 360 (NGC 3640 Group) LGG 292 (Virgo I Group) LGG 360 (NGC 3640 Group) LGG 360 (NGC 364	Parameter	NGC 3610	NGC 3640	NGC 4382	NGC 5322	NGC 7626
LGG 234 (NGC 3642 Group) LGG 233 (NGC 3640 Group) LGG 292 (Virgo I Group) LGG 234 (NGC 3640 Group) LGG 292 (Virgo I Group) LGG 294 (NGC 3640 Group) LGG 292 (Virgo I Group) LGG 294 (NGC 3640 Group) LGG 295 (Virgo I Group) LGG 295 (Virgo I GG 295 (Virgo I	Hubble type (RC3)	E5:	E3	SA(s)0+pec	E3-4	E1 pec
7.6 6.85 6.85 LGG 234 (NGC 3642 Group) LGG 233 (NGC 3640 Group) LGG 292 (Virgo I Group) 126 1997 Dec 3 1997 Dec 3 1997 Dec 3 1997 Dec 3 1787 1314 760 1516-2090 1044-1616 491-1061 11h18m25*9, +38°47'14" 11h21m06*8, +03°14" 12h25m24*7, +18°11/27" 2h 32m 2h 22m 1h57m 1h57m 1h57m 2h 32m 1331+305 1331+305 1206+642 1120+143 1254+116 1206+642 1120+143 1331+305 3.25 63 63 63 63 60 60 749" 62" x 49" 54" x 50"	Distance ^b (Mpc)	29.2	24.2	16.8	31.6	45.6
LGG 234 (NGC 3642 Group) LGG 233 (NGC 3640 Group) LGG 292 (Virgo I Group) 1 126 1997 Dec 3 1997 Dec 3 1997 Dec 3 1997 Dec 3 1787 1516–2090 1044–1616 491–1061 11h18m25*9, +38°47'14" 11h21m06*8, +03°14" 12h25m24*7, +18°11'27" 2h 32m 1331+305 1331+305 1331+305 1206+642 1120+143 1254+116 1206+642 1120+143 1331+305 3.25 63 63 63 63 64" × 49" 62" × 49" 66" × 49" 62" × 49"	Fine-structure index, c Σ	7.6	6.85	6.85	2.00	2.60
$\begin{array}{cccccccccccccccccccccccccccccccccccc$	Environment ^d	LGG 234 (NGC 3642 Group)	LGG 233 (NGC 3640 Group)	LGG 292 (Virgo I Group)	LGG 360 (NGC 5322 Group)	LGG 473 (Pegasus Group)
1997 Dec 3 1997 Dec 3 1997 Dec 3 1787 1314 1516–2090 11h18 ^m 25;9, +58°47′14" 11h21 ^m 06;8, +03°14" 2h 22m 1331+305 11206+642 11206+642 11206+642 11206+143 1331+305 3.25 63 63 10.4 10.4 10.4 10.4 10.4 10.4 10.4 1187 Dec 3 1760 491 Dec 3 1760 491 Dec 3 1760 1760 1760 1760 1760 1760 1760 1760	N, Known group members ^d	5	7	126	10	25
1787 1314 760 1516–2090 1044–1616 491–1061 11h18 ^m 25,9, +58°47′14" 11h21 ^m 06.8, +03°14" 12h25 ^m 24;7, +18°11′27" 2h 32m	Observed date	1997 Dec 3	1997 Dec 3	1997 Dec 3	1997 Dec 3	1997 Dec 7
1516–2090 1044–1616 491–1061 11h18 ^m 25,9, +58°47′14" 11h21 ^m 06.8, +03°14" 12h25 ^m 24;7, +18°11′27" 2h 32m 2h 2h 1h57m 1331+305 1331+305 1331+305 1206+642 1120+143 1254+116 1206+642 1120+143 1331+305 3.25 63 63 63 63 10.4 66" × 49" 62" × 49"	Velocity center ^e (km s ⁻¹)	1787	1314	092	1915	3423
11h18m25\$9,+\$8°47'14" 11h21m06\$8,+03°14" 12h25m24\$7,+18°111'27" 2h 22m 2h 32m 1331+305 1206+642 1310+143 1206+642 1120+143 1311+305 3.25 63 63 66" × 49" 66" × 49" 62" × 49" 62" × 49" 10.4	Velocity coverage ^f (km s ⁻¹)	1516–2090	1044–1616	491–1061	1644–2218	3159–3729
2h 32m 2h 22m 1h 57m 1331+305 1331+305 1331+305 1206+642 1120+143 1254+116 1206+642 1120+143 1331+305 3.25 63 63 66	Phase center coordinates (J2000.0)	$11^{h}18^{m}25^{\circ}9, +58^{\circ}47'14''$	$11^{\text{h}}21^{\text{m}}06^{\text{s}}8, +03^{\circ}14'''$	$12^{h}25^{m}24^{s}7, +18^{\circ}11'27''$	$13^{h}49^{m}15^{s}6,+60^{\circ}11'''$	23 h0m42 °4, $+08^{\circ}13'02''$
$\begin{array}{cccccccccccccccccccccccccccccccccccc$	Time on source	2h 32m	2h 22m	1h57m	2h 22m	2h 11m
$\begin{array}{cccccccccccccccccccccccccccccccccccc$	Flux calibrator	1331+305	1331+305	1331+305	1331+305	0137+331
$\begin{array}{cccccccccccccccccccccccccccccccccccc$	Phase calibrator	1206 + 642	1120 + 143	1254+116	1411+522	2253+161
3.25 3.25 3.25 63 63 63 10.4 10.4 10.4 10.4 66" × 49" 62" × 49" 54" 50"	Bandpass calibrator	1206 + 642	1120 + 143	1331+305	1411+522	2253+161
63 63 63 10.4 10.4 10.4 $66'' \times 49''$ $62'' \times 49''$ $54'' \times 50''$	Bandwidth (MHz)	3.25	3.25	3.25	3.25	3.25
$\begin{array}{cccccccccccccccccccccccccccccccccccc$	Number of channels	63	63	63	63	63
. 66" × 49" 62" × 49" 54" × 50"	Channel spacing (km s ⁻¹)	10.4	10.4	10.4	10.4	10.5
200	Synthesized beam (major \times minor axis)	$66'' \times 49''$	$62'' \times 49''$	$54'' \times 50''$	$57'' \times 50''$	$55'' \times 49''$
0.00	rms noise (mJy beam ⁻¹)	09.0	0.63	0.65	0.58	0.46

^a Optical velocities for NGC 3610 and NGC 5322 are from the Updated Zwicky Catalog (Falco et al. 1999), those for NGC 4382 and NGC 7626, from Smith et al. 2000, and those for NGC 3640, from the

RC3.

**Distances taken from the Nearby Galaxy Catalog (Tully 1988), except for NGC 7626, for which the optical velocity from the RC3 is used, assuming a Hubble constant of $H_0 = 75 \,\mathrm{km \, s^{-1}}$ Mpc⁻¹.

**Distances taken from Table 1 of SS92.

**Distances taken from Table 1 of SS92.

**Distances Galaxy Group catalog (LGG), number of known group members taken from NED.

**The central velocity for the H I observations were based on the best available optical velocities at the time of the observations, which were from the RC3 for all galaxies except NGC 4382, which was taken from Binggeli, Sandage, & Tammann 1985.

**Velocity coverage from channels 3–57 of H I data cube.

TABLE 2 VLA H i Observations^a

Galaxy (1)	Hubble Type (2)	Field (3)	$V_{\text{opt}} \atop \text{(km s}^{-1}\text{)} $ (4)	$V_{\rm H}$ (km s ⁻¹) (5)	$ \begin{array}{c} \Delta W \\ (\text{km s}^{-1}) \\ (6) \end{array} $	dr (arcmin) (7)	ρ (kpc) (8)	$(S_{\rm H} \Delta v)$ (Jy km s ⁻¹) (9)	$M_{ m H} \ (M_{\odot}) \ (10)$
NGC 3610	E5:	NGC 3610	1696			0	0	< 0.04	$< 2 \times 10^{7}$
NGC 3640	E3	NGC 3640	1314			0	0	< 0.05	$< 1 \times 10^{7}$
N3640 comp ^b	Uncataloged	NGC 3640		1180	62	15.1	105	2.4	3.3×10^{8}
NGC 4382	S0+pec	NGC 4382	729			0	0	< 0.06	$< 1 \times 10^{7}$
VCC 0797	E?	NGC 4382	773			2.9	14	< 0.06	$< 1 \times 10^{7}$
NGC 4394	SBb	NGC 4382	922	915	165	7.6	37	7.2	4.8×10^{8}
IC 3292	dS0	NGC 4382	710			8.5	42	< 0.07	$< 1 \times 10^{7}$
NGC 5322	E3-E4	NGC 5322	1781			0	0	< 0.04	$< 2 \times 10^{7}$
MCG +10-20-039	Unclassified	NGC 5322		1870	100	10.9	100	0.43	1.0×10^{8}
UGC 8714	Im	NGC 5322	2044	2030	210	23.2	215	4.7	1.1×10^{9}
NGC 7626	E1 pec	NGC 7626	3433	3518	105	2.7	36	0.17	8.3×10^{7}
AGC 330257	Unclassified	NGC 7626	3470			3.9	52	< 0.04	$< 3 \times 10^{7}$
NGC 7631 ^c	Sb	NGC 7626	3754	>3700	>200	11.0	145	>1.9	$>9.3 \times 10^{8}$
NGC 7623	S0 ⁰ :	NGC 7626	3739			11.1	145	< 0.05	$< 5 \times 10^{8}$
UGC 12510	E	NGC 7626	3542			15.8	210	< 0.08	$< 8 \times 10^{8}$

Notes.—Col. (4): Optical radial velocity from NED; col. (5): velocity centroid of H I line; col. (6): velocity width, calculated from intensity-weighted velocity map with no correction for inclination; col. (7): separation from targeted elliptical galaxy in arcminutes; col. (8): separation from targeted elliptical galaxy, assuming both systems lie at the distance given in Table 1; cols. (9)–(10): 6 σ limits, calculated from H I data cube smoothed to a velocity resolution of 42 km s⁻¹ and corrected for the primary-beam attenuation.

^b Uncataloged highly inclined low surface brightness companion at 11^h21^m51^s5, +03°24′17″ (J2000.0).

 $M_{\rm H\,I}$ is then in units of solar masses per beam. Where no detections were made, 6 σ upper limits were estimated from the velocity-smoothed data cube (i.e., over an H I line with of 42 km s⁻¹). H I masses or mass limits for each of the targets are listed in Table 2. Previous limits for these galaxies were typically $10^8-10^9~M_{\odot}$ from single-dish observations (Roberts et al. 1991). Limits from our VLA data are typically an order of magnitude lower.

4. RESULTS

In this section we summarize the properties of the observed galaxies and the results of the VLA observations. Galaxy classifications are from the RC3 (de Vaucouleurs et al. 1991), and distances are taken from the Nearby Galaxy Catalog (Tully 1988), which adopts $H_0 = 75 \text{ km s}^{-1} \text{ Mpc}^{-1}$. Group assignment was assessed using the Loose Galaxy Groups catalog (Garcia 1993, hereafter LGG), and the number of group members was evaluated via the NASA Extragalactic Database (NED). This information is summarized in Table 1.

We review the morphological properties of each system, listing the values for the fine-structure index and the "heuristic merger age," as tabulated by SS92. The heuristic merger age was calculated by matching a simple two-burst model of evolving stellar populations to the observed *UBV* colors (see SS92 for details). We also report spectroscopically determined age estimates available from the literature. In most cases, these are derived from single stellar populations (SSP) model fits to four or more spectroscopically derived metallicity- and age-dependent line indices (see, e.g., Gonzales 1993; Worthey 1994) and represent a luminosity-weighted mean age for the central stellar population. We briefly describe the results of previous H I observations (culled from the compilations of Huchtmeier & Richter

1989 and Martin 1998). We note that our VLA observations are most sensitive to narrow H I lines and may miss H I emission spread over a broad range of velocity. For such emission the large-beam single-dish limits are still relevant.

Finally, we present the results of our VLA H I mapping observations, which are summarized in Table 2. Figure 1 shows the integrated H I line maps for each of our five target galaxies contoured on a gray-scale representation of the optical light, taken from the Digital Sky Surveys (DSS). No H I was detected from within the optical bodies of any of the target galaxies. Only NGC 7626 shows evidence of some associated H I, out at projected radii from ~1.5 to 3′ from the galaxy center.

4.1. NGC 3610=UGC 6319

NGC 3610 is a member of the NGC 3642 Group (LGG 234), with five cataloged members. The NGC 3642 Group itself is a subgroup of the rich (N=170) Group 94 of Geller & Huchra (1983). The optical velocity from the Updated Zwicky Catalog (Falco et al. 1999) is 1696 km s⁻¹, whereas the H I observations were centered at the old RC3 value of 1787 km s⁻¹. This will not affect our detection sensitivity, since this difference is well within the observed band.

NGC 3610 has the highest value of Σ of any of the early types in the SS92 sample ($\Sigma=7.60$, heuristic merger age 4–7 Gyr). Only the young merger remnants NGC 3921 and NGC 7252 have higher values ($\Sigma=8.8$ and 10.1, respectively). The optical peculiarities include two or three shells, a central X-structure, plumes, and extraordinarily boxy outer isophotes (Forbes & Thomson 1992; Whitmore et al. 1997). While the outer isophotes are boxy, the inner isophotes are disky, because of an inner disk embedded within its spheroid (Scorza & Bender 1990). The system as a whole is rotationally flattened ($V/\sigma=1$; Scorza & Bender 1990), and the inner disk is kinematically distinct, with $V/\sigma=4.5$

^a Includes all H_I detections, as well as limits for all galaxies with known redshifts found in NED that fall within the primary beam (15' radius) and velocity coverage of the VLA observations.

c H I emission appears at the edge of the velocity coverage of the observations, so the high-velocity range of the H I emission is not measured.

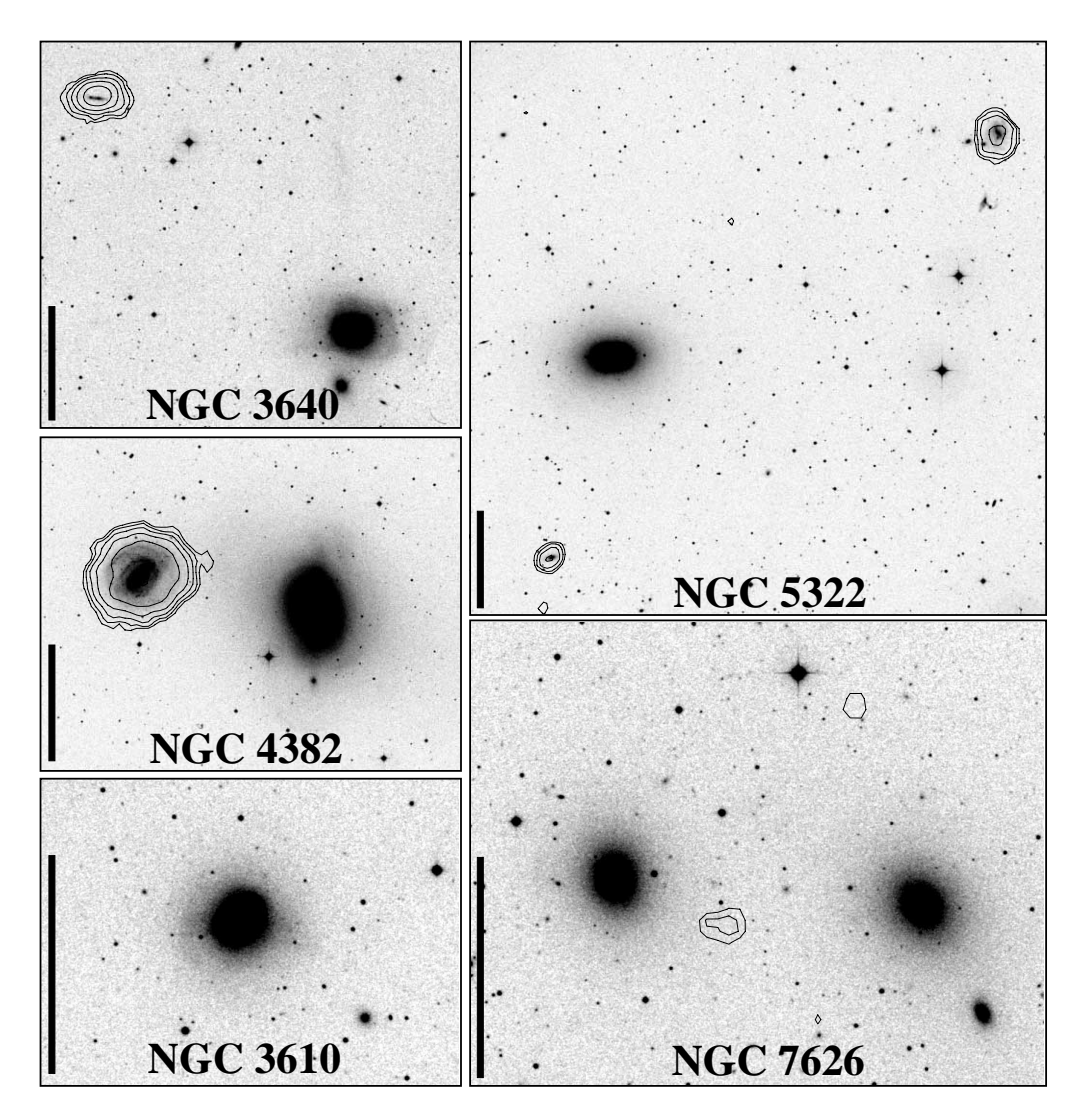


Fig. 1.—Montage of images for five E/S0 galaxies with fine structure. Contours of H I column density are drawn upon a gray-scale representation of the second-generation blue Digital Sky Survey images. Images are oriented such that north is up and east is to the left. Clockwise from top left are the fields for NGC 3640, 5322, 7626, 3610, and 4382. Starting contours are drawn at levels of 27.6, 25.8, 24.4, 0.0, and 24.5 Jy km s⁻¹, respectively, which corresponds to an H I column density of 1×10^{19} cm⁻². Successive contours are drawn a factor of 2 higher. The vertical bar in each frame is 5' long. Of these five galaxies, only NGC 7626 has H I directly associated with the targeted elliptical galaxy (see Table 2). In these images H I is detected in an uncataloged companion northeast of NGC 3640; MCG +10-20-039, a southern companion to NGC 5322; UGC 8714, a companion lying to the northwest of NGC 5322; a cloud lying west of NGC 7626; and NGC 4394, east of NGC 4382.

(Rix & White 1992). There are no color differences between the main body and the inner disk, and both seem to be composed of stars with similar ages (Scorza & Bender 1990; Whitmore et al. 1997). These observations are seen as evidence for an accretion, rather than a merger, origin (Scorza & Bender 1990; Silva & Bothun 1998b). However, the presence of an intermediate-age centrally concentrated globular cluster population (Whitmore et al. 1997, 2002) suggests a merger origin. The age of the red metal-rich globular cluster population is consistent with the broad band near-IR and optical age estimates of ~4–7 Gyr (Silva & Bothun 1998b; SS92).

Previous single-dish H I observations of NGC 3610 were conducted by Bieging (1978), who set a 3 σ upper limit of $\int S_{\rm H\,\textsc{i}} dv < 2.4$ Jy km s⁻¹ by using the Effelsberg 100 m telescope (8' HPBW). This places a limit on the H I mass to *B*-band luminosity of $M_{\rm H\,\textsc{i}}/L_B < 0.012~M_{\odot}~L^{-1}_{\odot}$. We find no H I emission within the primary beam of the VLA observations. The new H I limit is over an order of magnitude lower

than the previous limit $(M_{\rm H\ I}/L_B < 4 \times 10^{-4}\ M_{\odot}\ L^{-1}_{\odot})$. None of the other members of the LGG 234 Group fall within the primary beam (30' HPBW, or 130 kpc radius at the adopted distance of 29.2 Mpc) and velocity coverage of the present H I observations.

4.2. NGC 3640=UGC 6368

NGC 3640 is a member of NGC 3640 Group (LGG 233), with seven cataloged members. However, none of the other group members fall within the primary beam (105 kpc radius at the adopted distance of 24.2 Mpc) and velocity coverage of the present H I observations. The E pec galaxy NGC 3641 lies just 2.9 south of NGC 3640, but its velocity ($V_{\odot} = 1755 \,\mathrm{km\,s^{-1}}$) lies outside the observed band.

Along with NGC 4382, NGC 3640 has the second-highest value of the fine-structure index in the SS92 compilation ($\Sigma=6.85$, heuristic merger age 6–8 Gyr). It has a number of morphological peculiarities, including shells, boxy

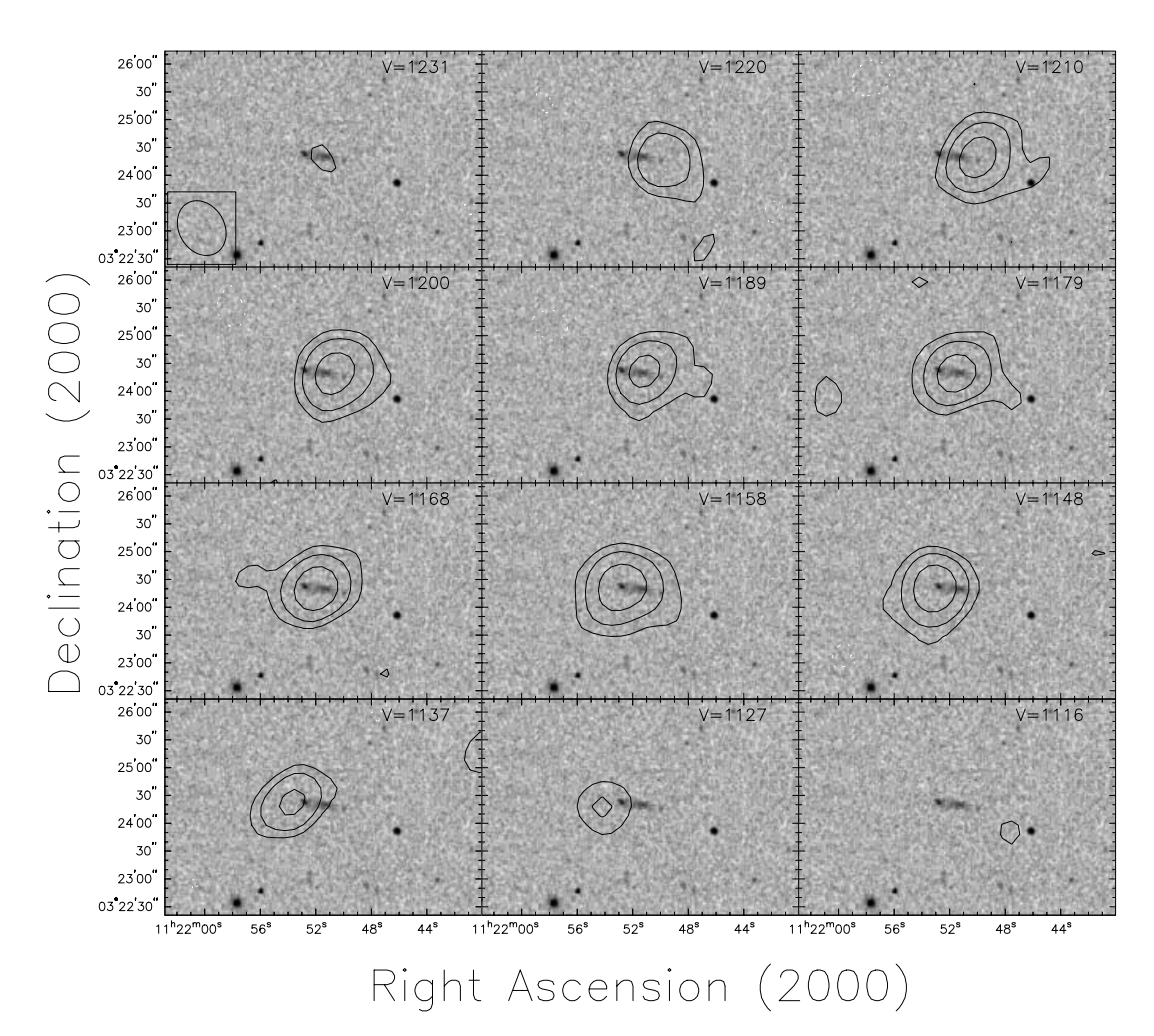


Fig. 2.—H I channel maps contoured upon a gray-scale representation of the DSS optical image for the H I-detected companion lying 15.1 (105 kpc) to the northeast of NGC 3640, at $11^{\text{h}}21^{\text{m}}51^{\text{s}}.5$, $+03^{\circ}24'17''$ (J2000.0). The heliocentric velocity of each channel is given at upper right in each panel, and the size of the synthesized beam $(62'' \times 49'' \text{ FWHM})$ is indicated by the inscribed ellipse at lower left in the first panel. Contours are drawn at levels of -3, 3, 6, and 12 times 1.2 mJy beam $^{-1}$, where the lowest contour corresponds to an H I column density of $1.4 \times 10^{19} \text{ cm}^{-2}$.

isophotes, a minor axis dust lane, and, like NGC 3610, it is a fast rotator ($V/\sigma=1.5$; Prugniel et al. 1988). The second-generation blue DSS image shows what appears to be a faint tidal tail extending directly to the north by about 10' (see Fig. 1). Prugniel et al. (1988) argue that NGC 3640 is a merger in progress, probably with a gas-poor system. Both the heuristic merger age derived by SS92 and the near-IR colors of NGC 3640 argue against a major starburst having occurred within the previous 3 Gyr (Silva & Bothun 1998a, 1998b).

NGC 3640 was previously searched for H I by Shostak, Roberts, & Peterson (1975), who set an upper limit of $\int S_{\rm H\,\textsc{i}} dv < 2.9 \,\mathrm{Jy~km~s^{-1}}$ by using the NRAO 300 ft (10 m) telescope (9'.3 HPBW), and by Lake & Schommer (1984), who set an upper limit of $\int S_{\rm H\,\textsc{i}} dv < 0.6 \,\mathrm{Jy~km~s^{-1}}$ by using the 305 m dish at Arecibo (3'.3 HPBW). This places a limit on the H I mass to *B*-band luminosity of $M_{\rm H\,\textsc{i}}/L_B < 0.003 \,M_{\odot}\,L^{-1}_{\odot}$.

We detect no H I emission associated with NGC 3640 $M_{\rm H\,I}/L_B < 6\times 10^{-4}~M_\odot~L^{-1}_\odot$). While none of the other members of the LGG 233 Group fall within our VLA settings, we do detect H I in an uncataloged galaxy lying 15'.1 (105 kpc) to the northeast at $11^{\rm h}21^{\rm m}51^{\rm s}5$, $+03^{\circ}24'17'$ (J2000.0). The integrated H I emission is contoured on the

DSS image in Figure 1, and the H I channel maps of the emission are given in Figure 2. From the DSS image, the companion appears to be a highly inclined low surface brightness dwarf spiral galaxy, and the H I kinematics are characteristic of regular disk rotation. The total detected H I flux, after correction by primary-beam attenuation, is 2.4 Jy km s⁻¹, corresponding to an H I mass of 3.3×10^8 M_{\odot} , assuming the companion lies at the distance of NGC 3640 listed in Table 1.

There is an unresolved radio continuum source that lies 47" to the southeast of NGC 3640, outside its main body, but within the fainter optical isophotes, with a flux of 41 mJy at 1.4 GHz. There is no optical counterpart on the DSS image, and this is probably a background radio source.

4.3. NGC4382=M85=UGC7508

NGC 4382 is a member of the Virgo I Group (LGG 292), with 126 cataloged members. Together with the elliptical VCC 797 (lying 2.9 to the south of NGC 4382) and the barred spiral NGC 4394 (lying 7.6 to the east), it forms Redshift Survey Compact Group 54 (Barton et al. 1996). The dS0 galaxy IC 3292 is also likely associated (see Table 2). This makes this association a compact group within a sub-

group of a moderately rich cluster. None of the other Virgo I Group members fall within the primary beam (73 kpc radius at the adopted distance of 16.8 Mpc) and velocity coverage of the present H I observations.

Along with NGC 3640, NGC 4382 has the second-highest value of the fine-structure index in the SS92 compilation ($\Sigma=6.85$, heuristic merger age 4–7 Gyr), with more than 12 irregular ripples, significant isophotal twists, and a plume to the north (Burstein 1979; SS92), and exhibits minor axis rotation (Fisher 1997). It has centrally enhanced H β and Mg₂ absorption, suggesting a relatively young (<3 Gyr) central population (Fisher, Franx, & Illingworth 1996; Terlevich & Forbes 2002, hereafter TF02).²

NGC 4382 has been observed numerous times with single-dish telescopes, with the best limit obtained by Burstein, Krumm, & Salpeter (1987), using Arecibo (3.3 HPBW) and sampling both the central position of NGC 4382 and pointings offset by 3' to each of the four compass points. No H I associated with NGC 4382 is detected, resulting in limits of $\int S_{\rm H\,\textsc{i}} dv < 0.2$ Jy km s⁻¹ and $M_{\rm H\,\textsc{i}} / L_B < 3 \times 10^{-4} M_{\odot} L^{-1}_{\odot}$. Burstein et al. claim a weak narrow H I feature in the pointing 3' south and close to the velocity of NGC 4382, which they tentatively associate with VCC 797.

We detect no H I emission associated with NGC 4382, to a limit of $\int S_{\rm H\,I} dv < 0.12$ Jy km s⁻¹, placing a limit of $M_{\rm H\,I}/L_B < 2 \times 10^{-4}~M_\odot~L^{-1}_\odot$. We do not confirm the tentative detection of H I with VCC 797, nor do we detect the dS0 IC 3292. We do detect $4.8 \times 10^8~M_\odot$ of H I in the barred spiral NGC 4394 (also detected by Burstein et al. and others). The gas in this galaxy forms an asymmetric ring, with the H I concentrated to the spiral features outside the bar (Fig. 3). The kinematics are very regular and symmetric, as seen in

the intensity-weighted velocity map (Fig. 3) and the channel maps (Fig. 4).

4.4. NGC 5322=UGC 8745

NGC 5322 is the dominant elliptical galaxy of the NGC 5322 Group (LGG 360), which has 10 cataloged members. However, none of the other group members fall within the primary beam (140 kpc radius at the adopted distance of 31.6 Mpc) and velocity coverage of the present H I observations (but see below). NGC 5322 has a recently updated optical velocity from the Updated Zwicky Catalog (Falco et al. 1999) of 1781 km s⁻¹, whereas the H I observations were centered at the old RC3 value of 1915 km s⁻¹. This difference is still well within the observed band.

NGC 5322 has less obvious optical peculiarities than the other systems in this sample ($\Sigma = 2.00$, heuristic merger age 5–8 Gyr). These include outer boxy and inner disky isophotes (Bender 1988). It also has peculiar stellar kinematics, with a small counterrotating disk embedded in a slowly rotating bulge (Bender 1988; Bender & Surma 1992; Rix & White 1992). There is a weak central radio source with symmetric jets aligned perpendicular to the central disk (Feretti et al. 1984), and the nuclear optical spectrum is characterized as a LINER. The central colors and [Mg/Fe] ratio of NGC 5322 suggest the presence of a 1-3 Gyr old central starburst population (Bender & Surma 1992; Silva & Bothun 1998a, 1998b). A luminosity-weighted age of 4.2 ± 0.6 Gyr was estimated from fitting SSP models to 20 central line strengths in NGC 5322 (Proctor & Sansom 2002), supporting the existence of a relatively young component.

NGC 5322 was previously searched for H I by using the NRAO Greenbank 140 ft (27 m) telescope (21' HPBW) by Knapp & Gunn (1982), obtaining an upper limit of

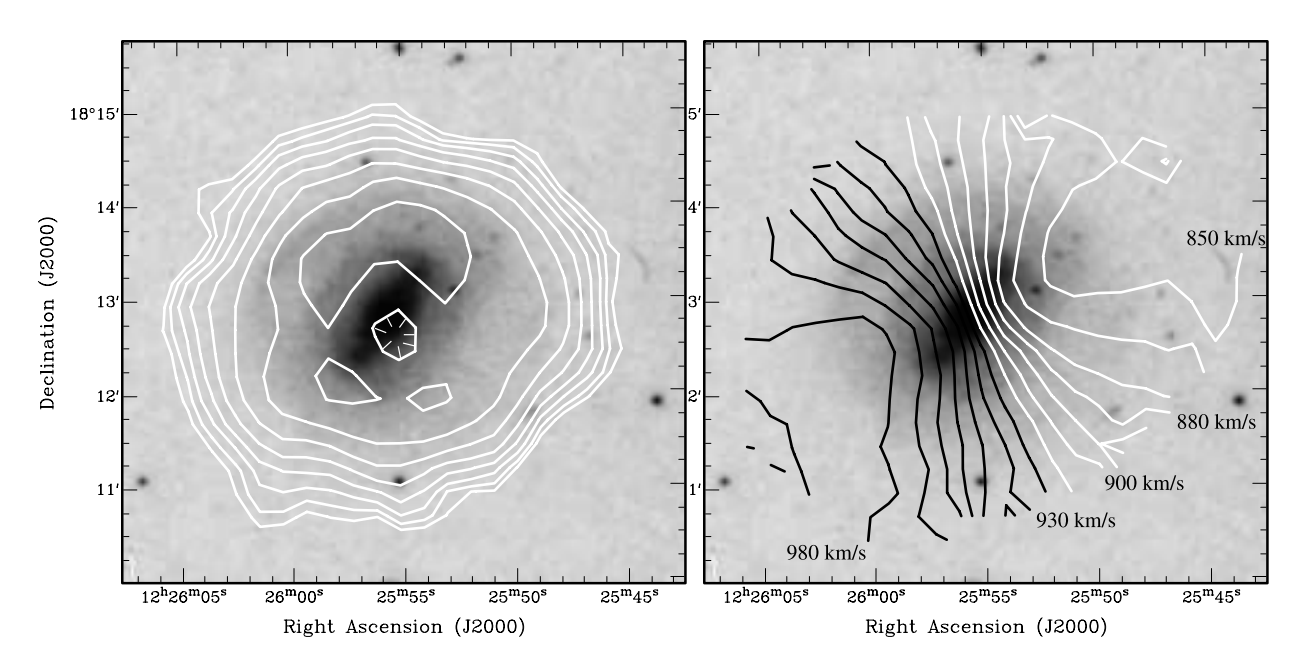


Fig. 3.—Integrated H I intensity (*left*) and intensity-weighted isovelocity field (*right*) contoured upon a gray-scale representation of the DSS optical image of NGC 4394, the barred companion east of NGC 4382. The integrated H I intensity is contoured at 48.9 Jy km s⁻¹ \times 2^{n/2} (n = 0, 1, 2, ...), where the lowest contour corresponds to an H I column density of 2×10^{20} cm⁻². The hatched contour represents a central depression in the H I distribution (see Fig. 4). The isovelocity field is contoured from 850 to 990 km s⁻¹ in steps of 10 km s⁻¹, with white contours representing blueshifted velocities relative to systemic, and black contours representing redshifted velocities.

 $^{^2}$ For Terlevich & Forbes see also http://www.astronomy.swin.edu.au/staff/dforbes/agecat.html.

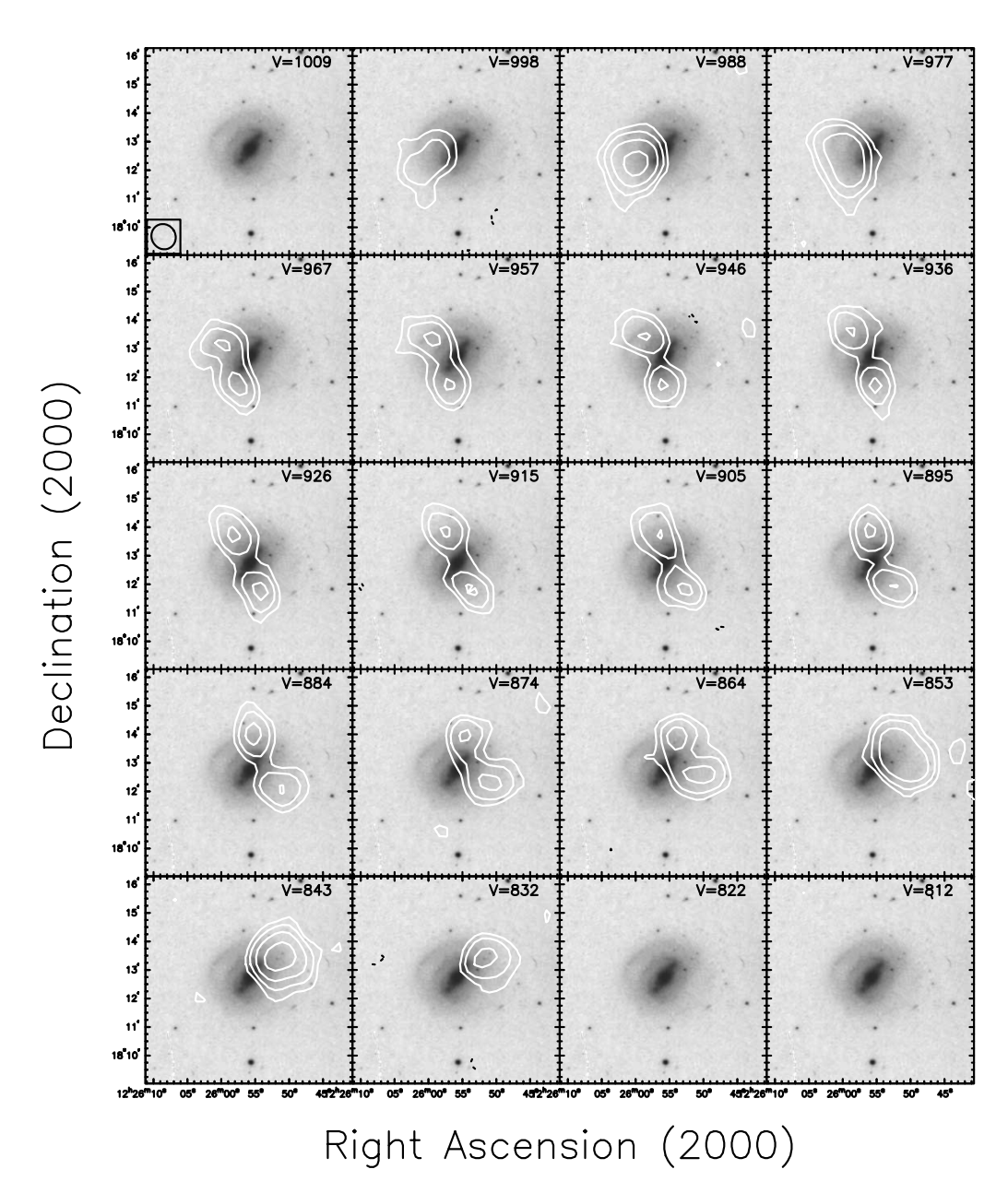


Fig. 4.—H I channel maps contoured upon a gray-scale representation of the DSS optical image for NGC 4394, the barred companion lying 7.6 (37 kpc) to the east of NGC 4382. The heliocentric velocity of each channel is given at upper right in each panel, and the size of the synthesized beam ($54'' \times 50''$ FWHM) is indicated by the inscribed ellipse at lower left in the first panel. Contours are drawn at levels of -3, 3, 6, 12, and 24 times 0.76 mJy beam $^{-1}$, where the lowest contour corresponds to an H I column density of 9.8×10^{18} cm $^{-2}$.

 $\int S_{\rm H\,{\scriptscriptstyle I}} dv < 8.5$ Jy km s⁻¹, resulting in the limit $M_{\rm H\,{\scriptscriptstyle I}}/L_B < 0.022\,M_{\odot}\,L^{-1}_{\odot}$.

We detect no H I emission associated with NGC 5322. The new H I limit is two orders of magnitude lower than the previous limit $(M_{\rm H\,I}/L_B < 2\times 10^{-4}~M_{\odot}~L^{-1}_{\odot})$. We do detect H I associated with two other nearby galaxies: MCG +10–20–039, an early-type disk system lying 10.9 (100 kpc) to the south, and UGC 8714, a dwarf irregular galaxy lying 23.2 (210 kpc) to the northwest. MCG +10–20–039 has no previously determined redshift, while UGC 8714 is a known member of the NGC 5322 Group. UGC 8714 was previously detected in the H I line by Schneider et al. (1992). See Figure 1 for the integrated H I contoured on the DSS image, Figure 5 for channel maps of MCG +10–20–039, and Figure 6 for channel maps of UGC 8714. The H I kine-

matics of MCG +10-20-039 do not appear very organized, but this may be a result of our relatively coarse spatial resolution. The H I kinematics of UGC 8714 are characteristic of an inclined rotating disk.

4.5. NGC 7626=UGC 12531

NGC 7626 is one of the two brightest elliptical galaxies in the Pegasus I Cluster, lying just 6!9 (90 kpc at the adopted distance of 45.6 Mpc) and 420 km s $^{-1}$ away from the dominant elliptical galaxy of that cluster, NGC 7619. Both galaxies are part of the Pegasus Group (LGG 473), with 25 cataloged members. However, the optical velocity of NGC 7619 ($V_{\odot}=3758~{\rm km~s^{-1}})$ and that of most of the other cluster members fall outside the high-velocity end of our bandpass ($V_{\odot}>3730~{\rm km~s^{-1}})$.

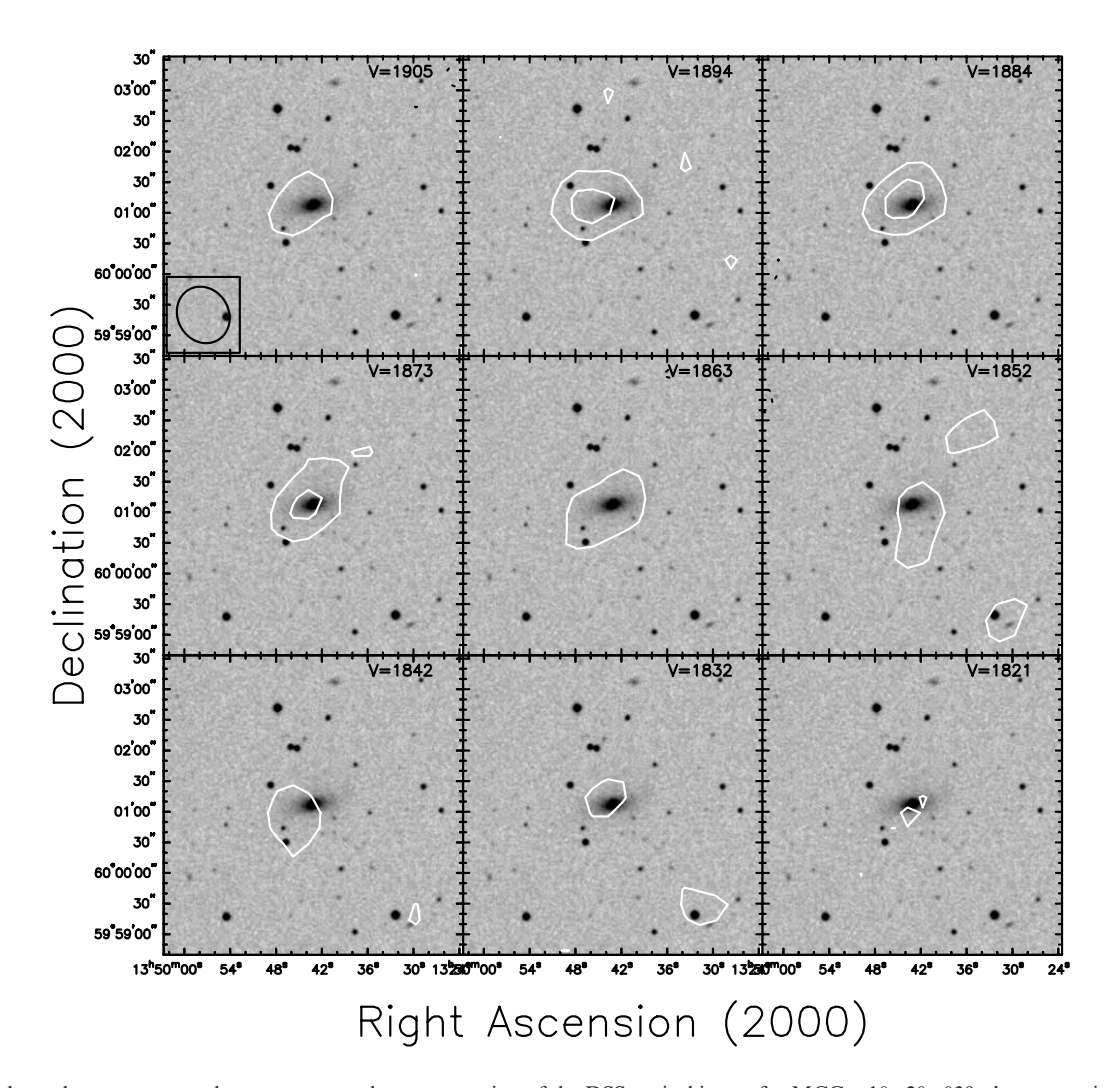


Fig. 5.—H I channel maps contoured upon a gray-scale representation of the DSS optical image for MCG +10-20-039, the companion lying 10.9 (100 kpc) to the south of NGC 5322. The heliocentric velocity of each channel is given at upper right in each panel, and the size of the synthesized beam $(57'' \times 50'')$ FWHM) is indicated by the inscribed ellipse at lower left in the first panel. Contours are drawn at levels of -3, 3, and 6 times 0.70 mJy beam $^{-1}$, where the lowest contour corresponds to an H I column density of 8.5×10^{18} cm $^{-2}$.

NGC 7626 has a modest amount of fine structure $(\Sigma = 2.60, \text{ heuristic merger age 7-9 Gyr})$. Its morphological peculiarities include outer and inner shells, a major axis dust lane, and an inner X-structure (Jedrzejewski & Schechter 1988; Forbes & Thomson 1992; Balcells & Carter 1993; Forbes, Franx, & Illingworth 1995). Hubble Space Telescope (HST) imaging reveals a symmetric dust feature within the inner 0".5 (Forbes et al. 1995; Carollo et al. 1997). This galaxy is noted for its very strange velocity field, which exhibits core rotation about an intermediate axis, and has shell-like regions of distinct kinematics around the core (Jedrzejewski & Schechter 1988; Balcells & Carter 1993; Longhetti et al. 1998). The kinematically decoupled core has an enhanced Mg₂ index relative to the outer regions (Davies, Sadler, & Peletier 1993), suggesting that its formation was accompanied by rapid star formation. Single-stellar population models of the core, inner, and global line indices suggest uniformly old ages for the central stellar populations of both NGC 7626 and NGC 7619 (7–12 Gyr; Gonzalez 1993; Longhetti et al. 2000; Trager et al. 2000; TF02).

NGC 7626 is a radio galaxy, with two symmetric jets on either side of a central core (Jenkins 1982; Birkinshaw & Davies 1985). Our radio continuum map is shown con-

toured on the DSS image in Figure 7. The lobes are edge-brightened and extend 8.0 (106 kpc) to the northeast and 6.3 (84 kpc) to the southwest. The core has a flux of 290 mJy at the observed sky frequency of 1404 MHz, while the entire radio structure has a total flux of 1.12 Jy. The radio jet is tilted by ~35° with respect to the dust lane imaged by *HST* (Forbes et al. 1995; Carollo et al. 1997). NGC 7619 has an unresolved radio continuum source with a flux of 25 mJy. NGC 7626 has a compact X-ray source at its center, most likely associated with the central engine, while NGC 7619 is a strong, extended X-ray source with an X-ray tail (Trinchieri, Fabbiano, & Kim 1997).

The region around and between NGC 7626 and NGC 7619 was mapped in the H I line by Kumar & Thonnard (1983) with Arecibo (3'.3 HPBW). No H I was detected at any of the eleven pointings, with resulting limit of $\int S_{\rm H\,I} dv < 1.1$ Jy km s⁻¹. A more stringent limit was set with the Effelsberg 100 m telescope (9'.3 HPBW) by Huchtmeier (1995) using a single pointing on NGC 7626, giving $\int S_{\rm H\,I} dv < 0.7$ Jy km s⁻¹ and $M_{\rm H\,I}/L_B < 0.007 \, M_{\odot} \, L^{-1}_{\odot}$.

We report a tentative detection of faint H I emission outside the optical body of NGC 7626. Figure 1 presents the integrated H I emission contoured upon the DSS image,

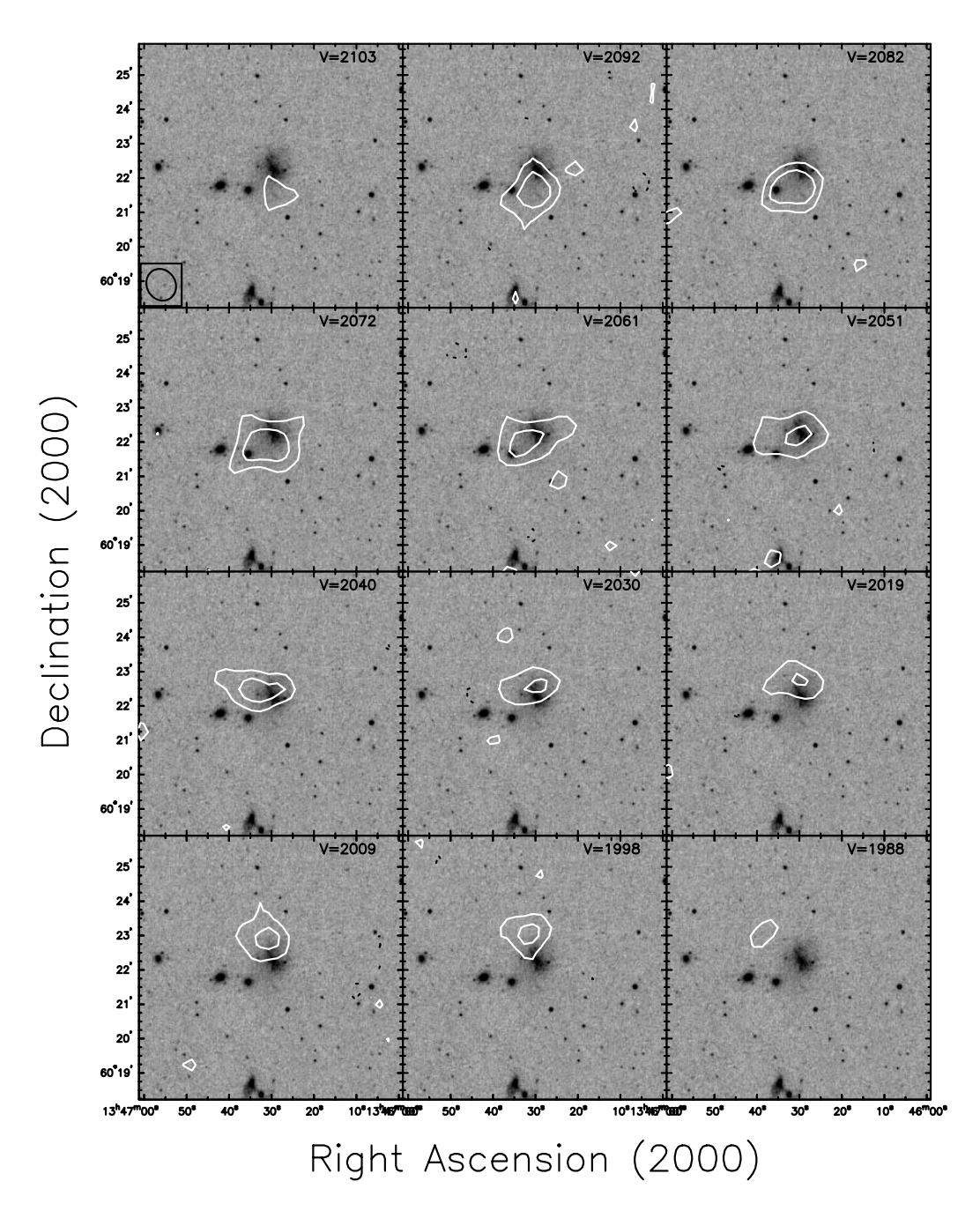


Fig. 6.—H I channel maps contoured upon a gray-scale representation of the DSS optical image for UGC 8714, the companion lying 23'2 (215 kpc) to the northwest of NGC 5322. The heliocentric velocity of each channel is given at upper right in each panel, and the size of the synthesized beam $(57'' \times 50'' \text{ FWHM})$ is indicated by the inscribed ellipse at lower left in the first panel. Contours are drawn at levels of -3, 3, and 6 times 2.9 mJy beam⁻¹, where the lowest contour corresponds to an H I column density of $3.5 \times 10^{19} \text{ cm}^{-2}$.

including both NGC 7626 (east) and NGC 7619 (west). Figure 7 shows a gray-scale image of the DSS with the integrated H I emission as thin contours along with thicker contours for the radio continuum emission. Figure 8 shows the channel maps over a field containing both NGC 7626 and NGC 7619. Since the single-beam single-channel flux is weak (with a peak line flux of 2 mJy beam⁻¹ or 4.3 σ), the channel maps do not convincingly show the H I emission. We therefore present two other figures: Figure 9, showing a position-velocity profile through the peak emission and parallel to the right ascension axis, and Figure 10, showing a spectrum extracted over the region containing the two features in the moment map. The optical velocity of NGC 7626

is indicated in both plots (Fig. 9, dashed line; Fig. 10, arrow). While the emission has a low signal-to-noise ratio, it appears in several adjacent channels. Still, the detection is considered tentative and should be confirmed by additional observations.

The neutral hydrogen emission lies between NGC 7626 and NGC 7619 in both space and velocity: the emission peak is at $23^{\rm h}20^{\rm m}32^{\rm s}.6$, $+08^{\circ}12'00''$ (J2000.0) and $V_{\odot}=3518$ km s⁻¹. This is 2!7 (36 kpc) and +85 km s⁻¹ from the optical center of NGC 7626 (Table 2), and 4!4 (59 kpc) and -240 km s⁻¹ from NGC 7619. The flux integrated over the spectrum of Figure 10 is 0.17 Jy km s⁻¹, which is consistent with the single-dish upper limits mentioned above. This flux cor-

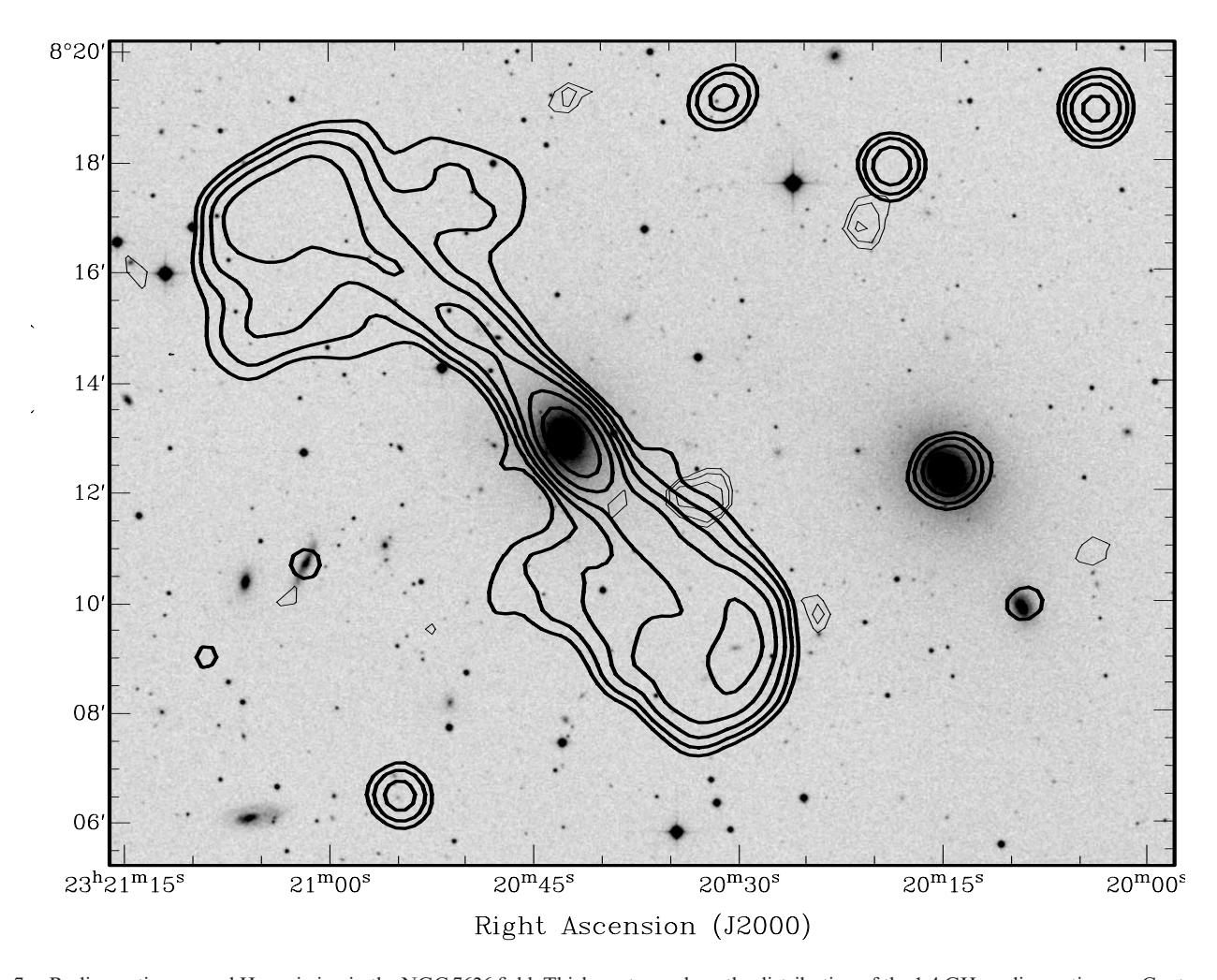


Fig. 7.—Radio continuum and H I emission in the NGC 7626 field. Thick contours show the distribution of the 1.4 GHz radio continuum. Contours start at 2 mJy beam $^{-1}$, with successive contours a factor of 2 higher than the previous contour. NGC 7619 lies directly to the west and is also a radio source, and NGC 7631 is the Sb galaxy lying directly to the east. Thin contours show the H I line emission integrated over the velocity range 3470–3600 km s $^{-1}$. Contours are drawn at levels of 1, 2, and 4 times 10 mJy beam $^{-1}$ km s $^{-1}$, where the lowest contour corresponds to an H I column density of 4 \times 10 18 cm $^{-2}$.

responds to an H I mass of $8.3 \times 10^7 M_{\odot}$ at the distance of NGC 7626. Curiously, the H I cloud lies just to the side of the radio jet (Fig. 7). A very similar situation occurs in the shell galaxy Cen A (NGC 5128; Schiminovich et al. 1994).

We detect H I in one other cluster member, the Sb galaxy NGC 7631, lying 11' (145 kpc) to east. This emission appears at the edge of our bandpass, so we do not map the full extent of H I line emission, and as such the H I flux and mass reported in Table 2 are lower limits. Channel maps for this galaxy are presented in Figure 11. The H I kinematics are characteristic of half of a rotating disk, with the higher velocity half falling outside our observing band. Three other cluster members fall within the primary beam and velocity coverage of our H I observations but are not detected (see Table 2).

5. DISCUSSION

5.1. H i in the NGC 7626 System

The detection of H I outside the optical body of NGC 7626 was something of a surprise. However, our earlier study on the global properties of the SS92 sample turned up a few shell systems with H I located outside their optical bodies (Table 2 of Sansom et al. 2000). Maps of these sys-

tems and other interesting examples appear in the H I Rogues Gallery (Hibbard et al. 2001b) in the category Peculiar Early Types with H I Outside Their Optical Body (objects 112–120 in the Rogues Gallery). This category is arranged in a sequence ranging from systems with abundant quantities of H I in the outer regions to systems with little or no H I in the outer regions, with NGC 7626 appearing near the end of the sequence.

There are a number of systems in this sequence that are quite similar to NGC 7626. Some specific examples are NGC 470/4, 1316, and 4125, and M86. NGC 474 is a spectacular shell system in the sample of SS92, with $\Sigma = 5.26$ and a heuristic merger age of 4–5 Gyr. There are H I clouds that appear to have been torn off the nearby Sb galaxy NGC 470 and distributed at several locations around the galaxy, but the H I does not appear to make it into the optical body of the galaxy (Schiminovich et al. 2001). Similarly, NGC 1316 (Fornax A) is a well-known peculiar system with many shells, ripples, and plumes, and with good evidence that it is a ≤3 Gyr merger remnant (Schweizer 1980; Goudfrooij et al. 2001a, 2001b). There are H I clumps around it that may have been torn from the nearby S0/a galaxy NGC 1317, but again these clouds avoid the main optical body of NGC 1316 (Horellou et al. 2001). NGC 4125 is a shell galaxy in the sample of SS92, with $\Sigma = 6.00$ and a heuristic merger

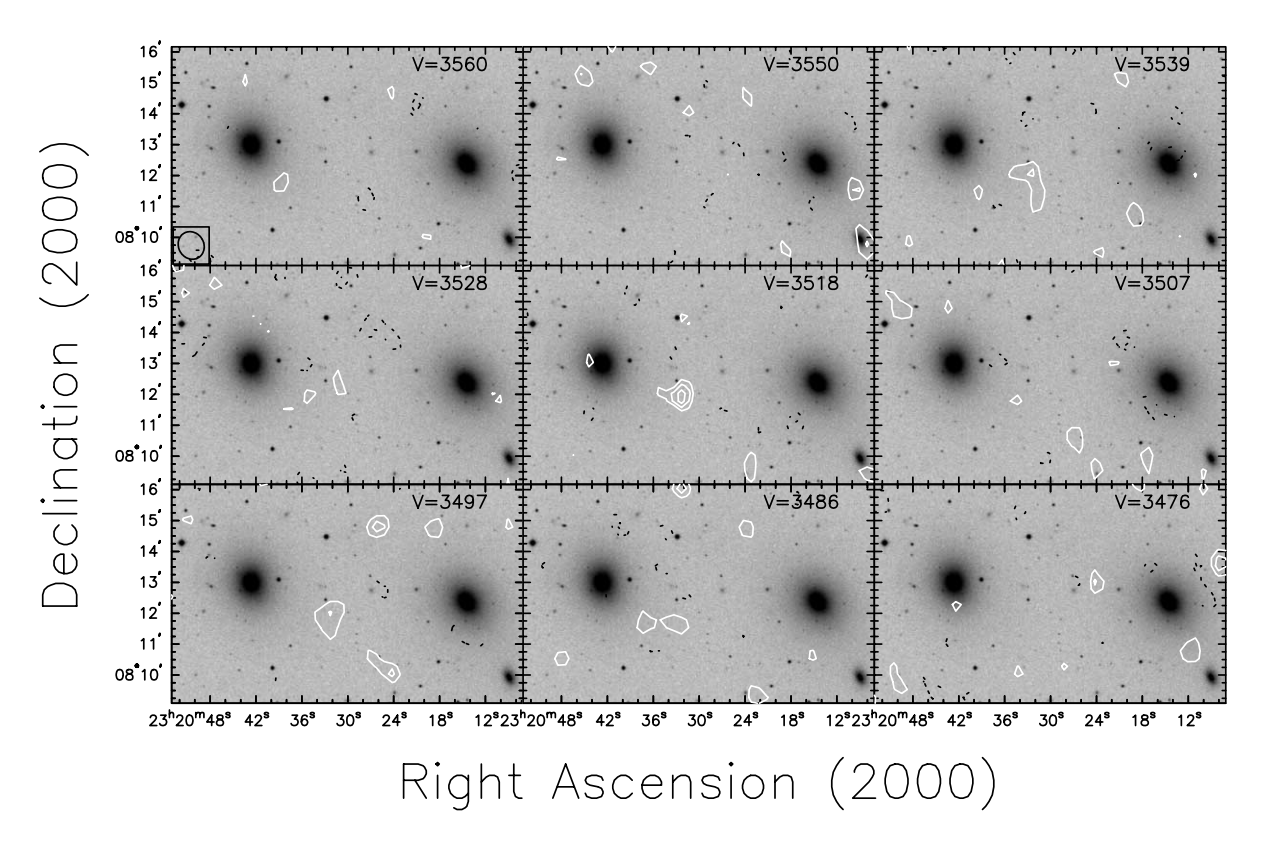


Fig. 8.—H I channel maps contoured upon an optical image from the DSS for NGC 7626 (east) and NGC 7619 (west). The heliocentric velocity of each channel is given at upper right in each panel, and the size of the synthesized beam $(55'' \times 49'' \text{ FWHM})$ is indicated by the inscribed ellipse at lower left corner in the first panel. Contours are drawn at levels of -3, -2, 2, 3, and 4 times 0.46 mJy beam⁻¹, where the lowest contour corresponds to an H I column density of 4×10^{18} cm⁻².

age of 6–8 Gyr. Unlike the other systems, it is apparently isolated. It has a few small H I clouds outside its optical body (Rupen, Hibbard, & Bunker 2001). M86 (a.k.a. NGC 4406) is a large early-type galaxy in the Virgo Cluster. It has an X-ray tail to the northwest and an H I cloud to the south, outside the main body of M86 (Li & van Gorkom 2001). NGC 7626 may also bear some resemblance to the radio galaxy Coma A, where H I has been detected in absorption against the radio lobes, some ~30 kpc from the galaxy center (Morganti et al. 2002).

While there are systems similar to NGC 7626, the nature of the intergalactic H I clouds is not at all clear. They could be diffuse remnant tidal debris that remains neutral only far outside the body of the elliptical galaxy, becoming photoionized by the stellar population at smaller radii (Hibbard, Vacca, & Yun 2000), or they could be a result of complex multiphase hydrodynamics, such as a jet-ISM, jet-ICM, or galaxy-ICM interaction. In this respect, X-ray imaging of the Pegasus Group would be very instructive.

5.2. H I in Fine-Structure Elliptical Galaxies

We expected a fair detection rate in these high Σ elliptical galaxies. This presumption was based primarily on two considerations: (1) peculiar E/S0 galaxies have a 45% H $_{\rm I}$ detection rate (Bregman, Hogg, & Roberts 1992; van Gorkom & Schiminovich 1997) and (2) the expectation that the highest Σ systems would be the youngest remnants of disk mergers and therefore most likely to still have gas-rich tidal debris. Therefore, we were somewhat surprised that only one of the five fine-structure galaxies that we targeted was detected in

H I. Moreover, the detected system, NGC 7626, is on the low end of the Σ scale, and we failed to detect H I in the three highest Σ systems in the compilation of SS92 (NGC 3610, 3640, and 4384).

While the number of systems that we observed in the present program is much too small to draw any statistical conclusions, in our previous study (Sansom et al. 2000) we examined all the available H I mapping data for galaxies in the lists of SS92. We found that 17/37 ($46\% \pm 16\%$) were detected in H I (i.e., the same fraction as found by Bregman et al. for peculiar E/S0s). The H I morphology suggests a tidal origin in all but three of these detections.

However, the SS92 compilation includes early types with a wide range of Σ . When plotting cold and hot gas properties versus Σ , we find no correlation besides the previously known tendency for recent (\lesssim 3 Gyr) merger remnants to be X-ray faint (Fabbiano & Schweizer 1995; Georgakakis et al. 2000; O'Sullivan et al. 2001).³

One possibility is that tidal H I does not survive for as long in the outer regions, as inferred from studies of young, more isolated merger remnants (Hibbard & Mihos 1995). Another possibility is that a high fine-structure index does not unambiguously identify recent disk-disk merger remnants. We look at each of these possibilities in turn.

Regarding the longevity of tidal material, in their dynamic study of the merger remnant NGC 7252 Hibbard & Mihos (1995) found that the outermost H I–rich material should remain at large radii from the remnant, evolving on

³ See also http://www.star.uclan.ac.uk/~aes/GALS/ISM.html.

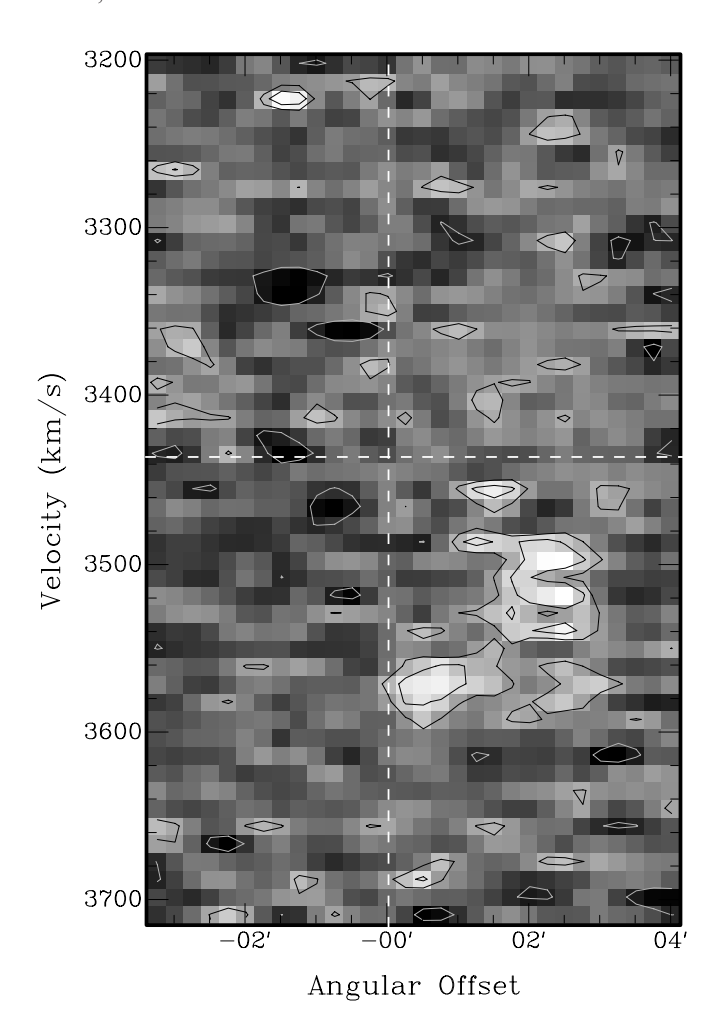


Fig. 9.—Position-velocity plot through the peak in the H I emission in the NGC 7626 field. The position angle of the simulated "slit" is 90° (i.e., parallel to the right ascension axis), centered at a declination of $+08^\circ 11'42''$ (J2000.0). The right ascension and systemic velocity of NGC 7626 are indicated by vertical and horizontal dashed lines, respectively. Contours are drawn at -1, 1, and 2 times 0.46 mJy beam $^{-1}$.

timescales of several gigayears. However, that study considered only the effects of gravity and did not address the survivability of the gas in its neutral form. As the tidal debris evolves, it becomes more diffuse. At low H I column densities, this gas may be susceptible to ionization by the intergalactic UV field (Hill 1974; Bland-Hawthorn & Maloney 1999) or even by the stellar population of the remnant (Hibbard et al. 2000). Perhaps more importantly, NGC 7252 is a relatively isolated system, while the five systems studied here are in groups or clusters. In such environments, the crossing times are of the same order as the timescale for tidal evolution, and it may be difficult for tidal H I to maintain a coherent morphology for very long (see also Verdes-Montenegro et al. 2001). We believe these effects contribute to the lack of detectable tidal H I in the targeted galaxies. In this case, such gas should give rise to extensive ionized halos around galaxies (Morris & van den Bergh 1994; Tadhunter

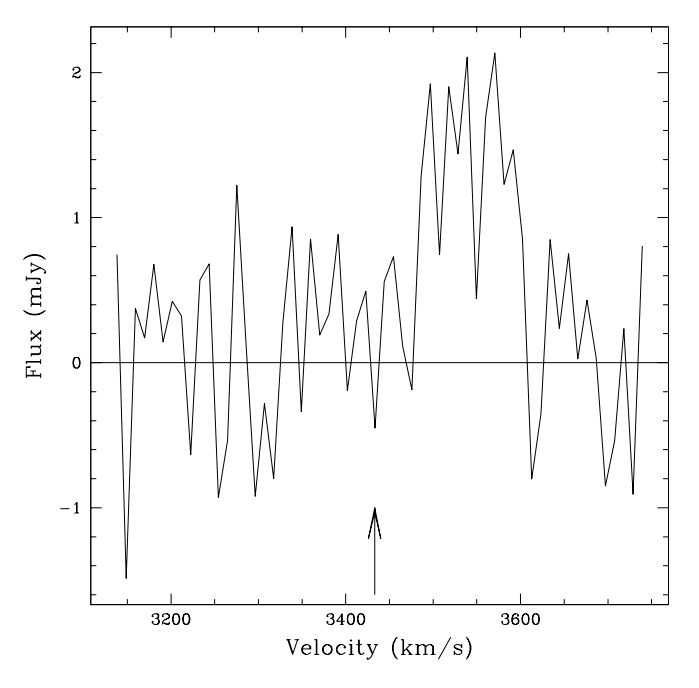


Fig. 10.—Integrated H $\scriptstyle\rm I$ line profile extracted over the region containing the two H $\scriptstyle\rm I$ features in the moment map. The velocity of NGC 7626 is indicated by the arrow.

et al. 2000), which may be detectable in absorption against background sources (e.g., Norman et al. 1996; Carilli & van Gorkom 1992). If we could accurately estimate the time since the merger, it would help evaluate the likelihood of this possibility.

Regarding the ability of a high fine-structure index to pick out the youngest merger remnant, we reevaluate the relationship between fine-structure index and population age indicators⁴ derived by SS92. The heuristic merger ages tabulated by SS92 were based on broadband *UBV* colors, which are not straightforward to interpret in terms of ages, because of age-metallicity degeneracies, nonsolar abundances and ratios, line emission, dust, frosting of a young population, etc. (see Worthey 1994 and Proctor & Sansom 2002 for discussions of some of these effects). Spectroscopic ages are now available using several line indices sensitive to both age and metallicity. We therefore reevaluate the relationship between fine-structure index and population age by using these new age indicators.

For our age indicators, we use the sample of early-type galaxies with uniform quality line strength data assembled from the literature by TF02, for which luminosity-weighted ages have been determined using the SSP models⁵ of Worthey (1994). We emphasize that these are not absolute ages, but age indicators: derived ages will differ for different models, but the relative age ranking should be maintained (see TF02 for a discussion of these points). We therefore do not augment this sample by including galaxies with merger ages estimated by different methods. Figure 12 shows how the fine-structure index compares with the logarithm of the spectroscopically determined ages [log(Age_{SP})] for the 26

⁴ Here we make the usual assumption that disk-disk mergers must be accompanied by a significant burst of star formation, lowering the luminosity-weighted mean age of the central stellar population. This is a gross simplification, since merger-induced star formation histories are likely quite complex. The derived ages should be considered as age indicators, rather than actual ages.

 $^{^5}$ We note that the TF02 line indices have been converted to measurements within the inner $R_e/8$ of the systems, where R_e is the effective radius of the galaxy, and therefore are most sensitive to the ages of the central stellar population.

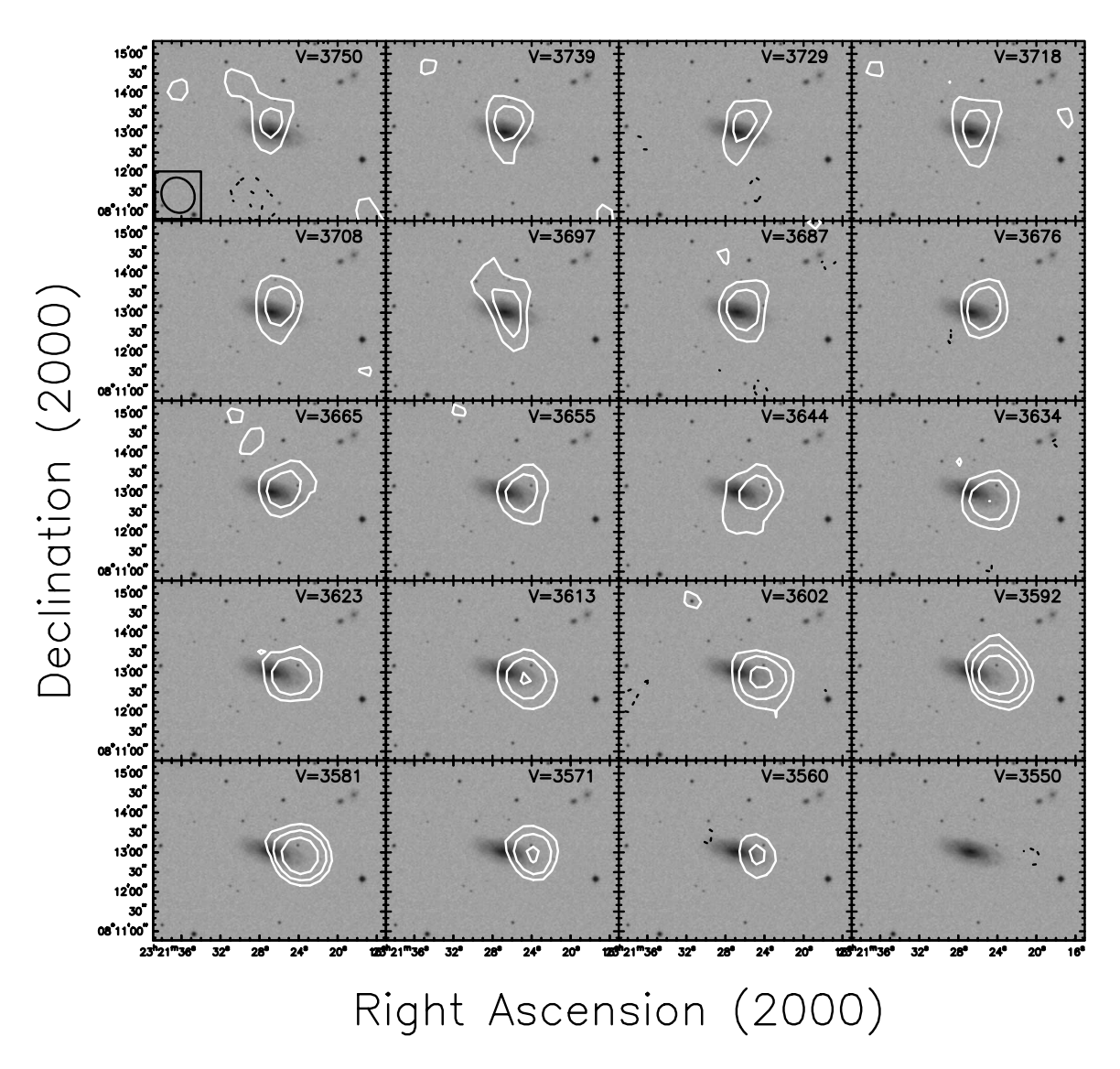


Fig. 11.—H I contours upon optical image from the DSS for H I channel maps contoured upon a gray-scale representation of the DSS optical image for NGC 7631, the companion lying 11' (145 kpc) to the east to NGC 7626. The heliocentric velocity of each channel is given at upper right in each panel, and the size of the synthesized beam (55" \times 49" FWHM) is indicated by the inscribed ellipse at lower left in the first panel. Contours are drawn at levels of -3, 3, 6, and 12 times 0.64 mJy beam $^{-1}$, where the lowest contour corresponds to an H I column density of 8.2×10^{18} cm $^{-2}$.

galaxies in the TF02 sample that also have fine structure quantified by SS92.

A statistical test of Σ and Age_{SP} for these 26 systems shows that they are highly anticorrelated (Spearman rankorder correlation coefficient $r_s = -0.70$). However, the correlation drops when the young merger remnants NGC 3921 and NGC 7252 are dropped from the sample ($r_s = -0.62$). Unlike the other systems in the SS92 sample, these two systems were included based on their status as known merger remnants. Further analysis indicates that most of the anticorrelation between Σ and Age_{SP} comes from systems with high Σ (\gtrsim 4) and young ages (\lesssim 3 Gyr; $r_s = -0.83$); the rank-order correlation coefficient drops to $r_s = -0.14$ for systems with lower Σ and higher Age_{SP}. Therefore, the apparent anticorrelation may be due to the purposeful inclusion of the well-known merger remnants NGC 7252 and NGC 3921 by both SS92 and TF02 at the high Σ , low spectroscopic age end and to the very few systems with a fine-structure index in the range $6 \lesssim \Sigma \lesssim 8$. Indeed, three of our systems fall within the range: NGC 3610, 3640, and

4382 (Table 1). NGC 4382 is one of the points in the plot, while NGC 3610 and NGC 3640 would lie well above the apparent relationship if the age indicators given in § 4 are taken (i.e., 4–7 Gyr for NGC 3610, and 6–8 Gyr for NGC 3640). So while Figure 12 reinforces the use of fine structure for tracking dynamically young remnants, it would be more reassuring to have more objects with a high fine structure and to have better age indicators than luminosity-weighted mean ages

In conclusion, we cannot say unambiguously that the five fine-structure elliptical galaxies studied here are King gap objects (i.e., evolved remnants of major disk-disk mergers). They may indeed be the result of gas-rich mergers, but evolved enough that any tidal gas that was thrown out during the encounter has fallen back, dispersed, or been converted to other forms. However, they may have had quite different histories, including minor mergers or major mergers of gas-poor progenitors. Together, these results suggest that progenitor type, encounter geometry, and local environment may all play an important role in the expected

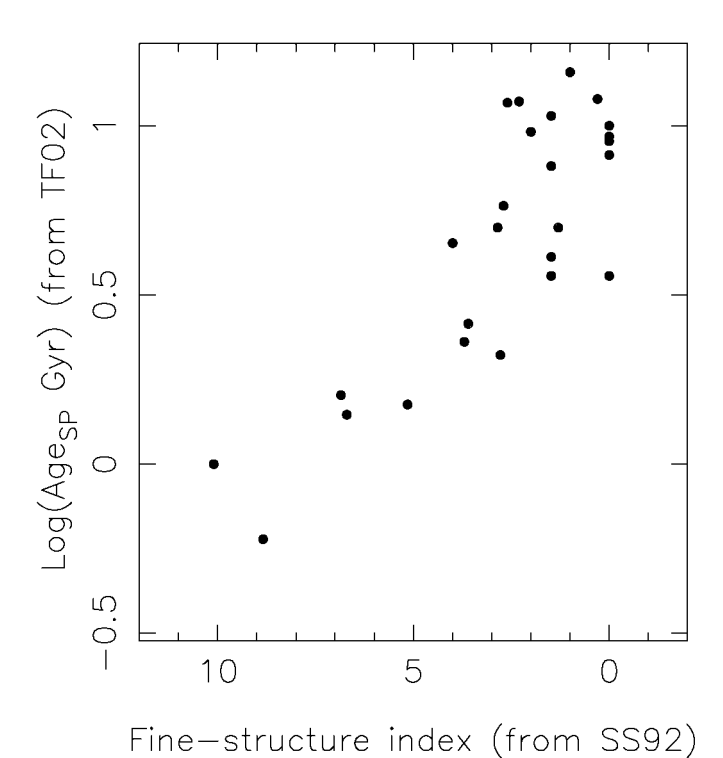


Fig. 12.—Logarithm of the spectroscopically determined age from TF02 (Age_{SP}), derived using SSP fits to H β and [MgFe] (combination of three) indices, vs. the morphological fine-structure index from SS92 (Σ), for the 26 galaxies common to the two samples.

postmerger evolution and that there is not one simple path from disk mergers to old elliptical galaxies (see also Hibbard et al. 2001b; Verdes-Montenegro et al. 2001). These possibilities can be constrained only by investigating young objects in the so-called King gap. To this end, Figure 12 offers some hope. Clearly, interacting systems may evolve in many ways in this plane, depending on what merged and how many stars, if any, were made during the interaction. Less drastic interacting histories may leave remnants anywhere along the right-hand side of this plot, making it harder to determine the origin of such systems. However, major mergers of gas-rich systems *must* evolve from lower left to upper right in the plot.

It is not clear *how* remnants will evolve in this plane or whether Σ and spectroscopically determined SSP ages are the best parameters to evaluate: Σ may not properly capture the dynamical evolution of the optical peculiarities and, given the range of possible progenitors and encounter geometries, perhaps no single parameter can; additionally, mergers of gas-rich systems may have complicated star formation histories (e.g., Mihos & Hernquist 1996) that are poorly constrained by simple stellar population models (see also Liu & Green 1996), and luminosity-weighted mean population ages may be only roughly related to the time since the latest merger event (Hibbard et al. 2001a). But the above considerations reinforce the suggestion of SS92 that signs of both dynamical youth and a youthful population should be used to identify the youngest King gap objects.

6. SUMMARY

We detected neutral hydrogen in the vicinity of four of the five fine-structure E/S0 galaxies that we observed with the VLA D array. In only one case is the H I directly associated with the targeted elliptical galaxy. For this one case, NGC 7626, there is a tentative detection of H I outside the optical body of the galaxy. This system contains a kinematically distinct core, but no obvious signs of being a recent merger, and its stellar population is uniformly old (at least as indicated by SSP determined ages). Therefore the origin of the H I is unclear, but similar systems are known from the literature.

Combining the present results with the analysis of Sansom et al. 2000, we find that galaxies with a large value of the fine-structure parameter, Σ , are no more likely to be detected in H I than those with a low value of Σ . This suggests that if the high Σ elliptical galaxies are aged remnants of disk-disk mergers, their tidal H I did not survive longer than a few gigayears. This may be due to the short crossing time in the group environment and/or due to ionization of the H I as it becomes more diffuse. This gas would contribute to a very diffuse neutral or ionized halo around the remnants.

Given these results, we conclude that the most promising way to constrain the observational characteristics of aged remnants of *gas-rich* mergers would be to target younger King gap objects (ages ≤ 2 Gyr) that contain signatures of both a dynamical youth and a youthful central stellar population. A growing population of objects is being identified, both by the appearance of optical and gaseous tidal features (e.g., Schiminovich et al. 2001; Chang et al. 2001; Hibbard et al. 2001b) and by spectroscopic studies of peculiar or normal early-type galaxies (e.g., Bergvall, Ronnback, & Johansson 1989; Oegerle, Hill, & Hoessel 1991; Zabludoff et al. 1996; Longhetti et al. 1998, 2000; Hau, Carter, & Balcells 1999; Trager et al. 2000; Georgakakis et al. 2001; TF02; Proctor & Sansom 2002).

Once a population of recent merger remnants is identified, they would enable us to judge the appearance of merger remnants at ages of ≥ 2 Gyr. By examining the cold gas content and distribution, global colors and line indices, inner/outer color differences, and light profiles of such systems, we could evaluate whether they are likely to evolve into normal elliptical galaxies or if instead they will leave long-lived signatures of their merger origin (Mihos & Hernquist 1994; Hibbard & Yun 1999; van den Marel & Zurek 2000; Mihos 2001). By identifying the expected observational signatures along the postmerger path we may ultimately be able to determine the fraction of the elliptical galaxy population that had a merger origin.

Our thanks to the staff at the VLA for their help in obtaining these observations and for help during our preliminary analysis. We thank F. Schweizer, J. van Gorkom, and D. Schiminovich for many fruitful conversations and for comments on earlier drafts of this paper.

The VLA of the National Radio Astronomy Observatory is operated by Associated Universities, Inc., under cooperative agreement with the National Science Foundation. This research has made use of the NASA/IPAC Extragalactic Database (NED), which is operated by the Jet Propulsion Laboratory, California Institute of Technology, under contract with the National Aeronautics and Space Administration. Optical images were taken from the Digitized Sky Surveys, produced at the Space Telescope Science Institute under government grant NAG W-2166. The images of these surveys are based on photographic data obtained using the Oschin Schmidt Telescope on Palomar Mountain.

REFERENCES

Balcells, M., & Carter, D. 1993, A&A, 279, 376

Balcells, M., van Gorkom, J. H., Sancisi, R., & del Burgo, C. 2001, AJ, 122,

Barnes, J. E., & Hernquist L. 1991, ApJ, 370, L65

Barton, E., Geller, M. J., Ramella, M., Marzke, R. O., & Da Costa, L. N. 1996, AJ, 112, 871 Bender, R. 1988, A&A, 202, L5

Bender, R., 360, A&A, 202, L3 Bender, R., & Surma, P. 1992, A&A, 258, 250 Bergyall, N., Ronnback, J., & Johansson, L. 1989, A&A, 222, 49 Bieging, J. H. 1978, A&A, 64, 23

Binggeli, B., Sandage, A., & Tammann, G. A. 1985, AJ, 90, 1681 Birkinshaw, M., & Davies, R. L. 1985, ApJ, 291, 32 Bland-Hawthorn, J., & Maloney, P. R. 1999, ApJ, 510, L33 Bregman, J. N., Hogg, D. E., & Roberts, M. S. 1992, ApJ, 387, 484 Briggs, D. 1995, Ph.D. thesis, New Mexico Institute of Mining and

Technology Burstein, D. 1979, ApJS, 41, 435

Burstein, D., Krumm, N., & Salpeter, E. E. 1987, AJ, 94, 883 Carilli, C. L., & van Gorkom, J. H. 1992, ApJ, 399, 373 Carollo, C. M., Danziger, I. J., Rich, R. M., & Chen, X. 1997, ApJ, 491,

Chang, T.-C., van Gorkom, J. H., Zabludoff, A. I., Zaritsky, D., & Mihos, J. C. 2001, AJ, 121, 1965

Davies, R. L., Sadler, E. M., & Peletier, R. F. 1993, MNRAS, 262,

de Vaucouleurs, G., de Vaucouleurs, A., Corwin, H. G., Jr., Buta, R. J., Paturel, G., & Fouqué, P. 1991, Third Reference Catalogue of Bright Galaxies (New York: Springer) (RC3)

Dupraz, C., & Combes, F. 1986, A&A, 166, 53

Fabbiano, G., & Schweizer, F. 1995, ApJ, 447, 572 Falco, E. E., et al. 1999, PASP, 111, 438

Feretti, L., Giovannini, G., Hummel, E., & Kotanyi, C. G. 1984, A&A,

Fisher, D. 1997, AJ, 113, 950

Fisher, D., Franx, M., & Illingworth, G. 1996, ApJ, 459, 110

Forbes, D., Franx, M., & Illingworth, G. 1995, AJ, 109, 1988 Forbes, D. A., & Thomson, R. C. 1992, MNRAS, 254, 723

Garcia, A. M. 1993, A&AS, 100, 47 (LGG) Geller, M. J., & Huchra, J. P. 1983, ApJS, 52, 61

Georgakakis, A., Forbes, D. A., & Norris, R. P. 2000, MNRAS, 318,

Georgakakis, A., Hopkins, A. M., Caulton, A., Wiklind, T., Terlevich, A. I., & Forbes, D. A. 2001, MNRAS, 326, 1431

Gonzalez, J. J. 1993, Ph.D. thesis, Univ. California Santa Cruz

Goudfrooij, P., Alonso, M. V., Maraston, C., & Minniti, D. 2001a, MNRAS, 328, 237

Hernquist, L., & Spergel, D. N. 1992, ApJ, 399, L117 Hibbard, J. E., Guhathakurta, P., van Gorkom, J. H., & Schweizer, F. 1994, AJ, 107, 67

Hibbard, J. E., & Mihos, J. C. 1995, AJ, 110, 140 Hibbard, J. E., Vacca, W. D., & Yun, M. S. 2000, AJ, 119, 1130 Hibbard, J. E., van der Hulst, J. M., Barnes, J. E., & Rich, R. M. 2001a, AJ,

Hibbard, J. E., & van Gorkom, J. H. 1996, AJ, 111, 655

Hibbard, J. E., van Gorkom, J. H., Rupen, M. P., & Schiminovich,
D. 2001b, in ASP Conf. Ser. 240, Gas and Galaxy Evolution, ed.
J. E. Hibbard, M. P. Rupen, & J. H. van Gorkom (ASP: San Francisco), 659

Hibbard, J. E., & Yun, M. S. 1999, ApJ, 522, L93

Hilloard, J. E., & Tuli, M. S. 1777, Ap., 322, 275
Hill, J. K. 1974, A&A, 34, 431
Horellou, C., Black, J. H., van Gorkom, J. H., Combes, F., van der Hulst, J. M., & Charmandaris, V. 2001, A&A, 376, 837
Huchtmeier, W. K. 1995, A&A, 286, 389
Huchtmeier, W. K., & Richter, O.-G. 1989, A General Catalog of H I Observations of Galaxies (New York: Springer)

Language P. L. 1988, Ap. 1, 330, 1.87

Jedrzejewski, R., & Schechter, P. L. 1988, ApJ, 330, L87

Jenkins, C. R. 1982, MNRAS, 200, 705 Knapp, G. R., & Gunn, J. E. 1982, AJ, 87, 1634 Kumar, C. K., & Thonnard, N. 1983, AJ, 88, 260 Lake, G., & Schommer, R. A. 1984, ApJ, 280, 107 Li, Y., & van Gorkom, J. H. 2001, in ASP Conf. Ser. 240, Gas and Galax: Evolution, ed. J. E. Hibbard, M. P. Rupen, & J. H. van Gorkom (ASP: San Francisco), 637

Lim, J., & Ho, P. T. P. 1999, ApJ, 510, L7 Liu, C. T., & Green, R. F. 1996, ApJ, 458, L63

Longhetti, M., Rampazzo, R., Bressan, A., & Chiosi, C. 1998, A&AS, 130,

2000, A&A, 353, 917

Malin, D. F. 1978, Nature, 276, 591 ———. 1979, Nature, 277, 279

Malin, D. F., & Carter, D. 1980, Nature, 285, 643

Malin, D. F., & Carter, D. 1983, ApJ, 274, 534 Martin, M. C. 1998, A&AS, 131, 73 Mihos, J. C. 2001, in ASP Conf. Ser. 240, Gas and Galaxy Evolution, ed. J. E. Hibbard, M. P. Rupen, & J. H. van Gorkom (ASP: San Francisco), 143

Mihos, J. C., & Hernquist, L. 1994, ApJ, 437, L47
——. 1996, ApJ, 464, 641
Miller, B. W., Whitmore, B. C., Schweizer, F., & Fall, S. M. 1997, AJ, 114, 2381

Morganti, R., Oosterloo, T. A., Tinti, S., Tadhunter, C. N., Wills, K. A., & van Moorsel, G. 2002, A&A, 387, 830 Morris, S. L., & van den Bergh, S. 1994, ApJ, 427, 696

Norman, C., Bowen, D. V., Heckman, T., Blades, C., & Danly, L. 1996, ApJ, 472, 73

Oegerle, W. R., Hill, J. M., & Hoessel, J. G. 1991, ApJ, 381, L9

O'Sullivan, E., Forbes, D. A., & Ponman, T. J. 2001, MNRAS, 324,

Proctor, R. N., & Sansom, A. E. 2002, MNRAS, 333, 517

Prugniel, P., Nieto, J.-L., Bender, R., & Davoust, E. 1988, A&A, 204,

Quinn, P. J. 1984, ApJ, 279, 596

Read, A. M., & Ponman, T. J. 1998, MNRAS, 297, 143 Reid, N., Boisson, C., & Sansom, A. E. 1994, MNRAS, 269, 713 Rix, H.-W., & White, S. D. M. 1992, MNRAS, 254, 389

Roberts, M. S., Hogg, D. E., Bregman, J. N., Forman, W. R., & Jones, C. 1991, ApJS, 75, 751 Rupen, M. P. 1999, in ASP Conf. Ser. 180, Synthesis Imaging in Radio

Astronomy, ed. G. B. Taylor, C. L. Carilli, & R. A. Perley (San Francisco: ASP), 229

Rupen, M. P., Hibbard, J. E., & Bunker, K. 2001, in ASP Conf. Ser. 240, Gas and Galaxy Evolution, ed. J. E. Hibbard, M. P. Rupen, & J. H. van Gorkom (ASP: San Francisco), 864

Sansom, A. E., Hibbard, J. E., & Schweizer, F. 2000, AJ, 120, 1946 Schiminovich, D. 2001, in ASP Conf. Ser. 240, Gas and Galaxy Evolution, ed. J. E. Hibbard, M. P. Rupen, & J. H. van Gorkom (ASP: San Francisco), 147

Schiminovich, D., van Gorkom, J. H., Dijkstra, M., Li, Y., Petric, A., & van der Hulst, J. M. 2001, in ASP Conf. Ser. 240, Gas and Galaxy Evolution, ed. J. E. Hibbard, M. P. Rupen, & J. H. van Gorkom (ASP: San Francisco), 864

Schiminovich, D., van Gorkom, J. H., van der Hulst, J. M., & Kasaw, S. 1994, ApJ, 423, L101

Schiminovich, D., van Gorkom, J. H., van der Hulst, J. M., & Malin, D. F. 1995, ApJ, 444, L77

Schneider, S. E., Thuan, T. X., Mangum, J. G., & Miller, J. 1992, ApJS, 81,5

Schweizer, F. 1980, ApJ, 237, 303
——. 1982, ApJ, 252, 455
——. 1996, AJ, 111, 109
——. 1998, in Saas-Fee Advanced Course 26, Galaxies: Interactions and Induced Star Formation, ed. R. C. Kennicutt, Jr., F. Schweizer, & J. E.

Barnes (Berlin: Springer), 105 Schweizer, F., & Ford, W. K., Jr. 1984, Lecture Notes in Physics 232, New Aspects of Galaxy Photometry, ed. J.-L. Nieto (Berlin: Springer),

Schweizer, F., Miller, B. W., Whitmore, B. C., & Fall, S. M. 1996, AJ, 112, 1839

Schweizer, F., & Seitzer, P. 1988, ApJ, 328, 88
——. 1992, AJ, 104, 1039 (SS92)
Schweizer, F., Seitzer, P., Faber, S. M., Burstein, D., Dalle Ore, C. M., & Gonzalez, J. J. 1990, ApJ, 364, L33
Scorza, C., & Bender, R. 1990, A&A, 235, 49
Schepter, C. S. Packett, M. S. & Patrons, S. D. 1075, AJ, 80, 581

Shostak, G. S., Roberts, M. S., & Peterson, S. D. 1975, AJ, 80, 581

Silva, D. R., & Bothun, G. D. 1998a, AJ, 116, 85

1998b, AJ, 116, 2793

Terlevich, A. I., & Forbes, D. A. 2002, MNRAS, 330, 547 (TF02)
Toomre, A. 1977, in The Evolution of Galaxies and Stellar Populations, ed.
B. M. Tinsley & R. B. Larson (New Haven: Yale Univ. Press), 401
Toomre, A., & Toomre, J. 1972, ApJ, 178, 623

Trager, S. C., Faber, S. M., Worthey, G., & Gonzalez, J. J. 2000, AJ, 119,

Trinchieri, G., Fabbiano, G., & Kim, D.-W. 1997, A&A, 318, 361

Tully, R. B. 1988, Nearby Galaxies Catalog (Cambridge: Cambridge Univ.

van den Marel, R. P., & Zurek, D. 2000, in ASP Conf. Ser. 197, Dynamics of Galaxies: From the Early Universe to the Present, ed. F. Combes, G. A. Mamon, & V. Charmandaris (San Francisco: ASP), 323

van Gorkom, J., & Schiminovich, D. 1997, in ASP Conf. Ser. 116, The Nature of Elliptical Galaxies, ed. M. Arnaboldi, G. S. Da Costa, & P. Saha (San Francisco: ASP), 310

Verdes-Montenegro, L., Yun, M. S., Williams, B. A., Huchtmeier, W. K., Del Olmo, A., & Perea, J. 2001, A&A, 377, 812 Whitmore, B. C., Miller, B. W., Schweizer, F., & Fall, S. M. 1997, AJ, 114,

1797 Whitmore, B. C., Schweizer, F., Kundu, A., & Miller, B. W. 2002, AJ, 124, 147

Worthey, G. 1994, ApJS, 95, 107 Yun, M. S., & Hibbard, J. E. 2001, ApJ, 550, 104 Zabludoff, A. I., Zaritsky, D., Lin, H., Tucker, D., Hashimoto, Y., Shectman, S. A., Oemler, A. A., & Kirshner, R. P. 1996, ApJ, 466, 104